NON-NORMALITY IN SCALAR DELAY DIFFERENTIAL EQUATIONS

A

THESIS

Presented to the Faculty

of the University of Alaska Fairbanks

in Partial Fulfillment of the Requirements

for the Degree of

MASTER OF SCIENCE

By

Jacob Nathaniel Stroh

Fairbanks, Alaska

December 2006

UMI Number: 1441029

Copyright 2006 by
Stroh, Jacob Nathaniel

All rights reserved.

INFORMATION TO USERS

The quality of this reproduction is dependent upon the quality of the copy
submitted. Broken or indistinct print, colored or poor quality illustrations and
photographs, print bleed-through, substandard margins, and improper
alignment can adversely affect reproduction.

In the unlikely event that the author did not send a complete manuscript
and there are missing pages, these will be noted. Also, if unauthorized
copyright material had to be removed, a note will indicate the deletion.

UMI®

UMI Microform 1441029
Copyright 2007 by ProQuest Information and Learning Company.
All rights reserved. This microform edition is protected against
unauthorized copying under Title 17, United States Code.

ProQuest Information and Learning Company
300 North Zeeb Road
P.O. Box 1346
Ann Arbor, MI 48106-1346

The aim of education is the knowledge, not of facts, but of values.

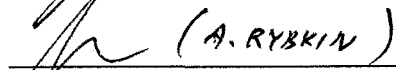~ William Seward Burroughs II

© 2006 Jacob Nathaniel Stroh

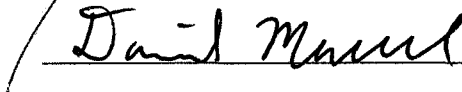# NON-NORMALITY IN SCALAR DELAY DIFFERENTIAL EQUATIONS
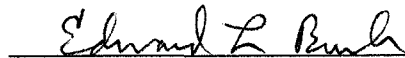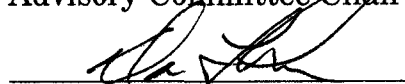
By

JACOB NATHANIEL STROH
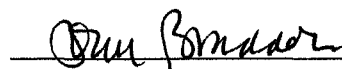
RECOMMENDED:

(A. RYBKIN)

Advisory Committee Chair

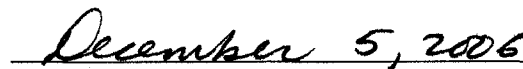Chair, Department of Mathematics and Statistics

APPROVED:

Dean, College of Natural Science and Mathematics

Dean of the Graduate School

December 5, 2006

Date

Abstract

Analysis of stability for delay differential equations (DDEs) is a tool in a variety of fields such as nonlinear dynamics in physics, biology, and chemistry, engineering and pure mathematics. Stability analysis is based primarily on the eigenvalues of a discretized system. Situations exist in which practical and numerical results may not match expected stability inferred from such approaches. The reasons and mechanisms for this behavior can be related to the eigenvectors associated with the eigenvalues. When the operator associated to a linear (or linearized) DDE is significantly non-normal, the stability analysis must be adapted as demonstrated here. Example DDEs are shown to have solutions which exhibit transient growth not accounted for by eigenvalues alone. Pseudospectra are computed and related to transient growth.

Table of Contents

List of Figures

Acknowledgments

I would like to first thank Dr. Edward Bueler for guiding this research and teaching me a lot of great mathematics through his frequent insightful rants. I would also like to thank the math faculty, especially committee members for making corrections. I am grateful to Dr. David Maxwell for volunteering his time for my exam preparation. Dr. John Gimbel also deserves praise for giving me my first 'C' in a math class. It is certainly worthwhile to be reminded that learning is more important than earning grades, and that it is often difficult to learn things which one finds disinteresting. Lastly, I must thank Dr. Alexei Rybkin for accepting me to the department, and to Dr. Dana Thomas: Thank you for additional funding, without which I may not have finished this degree.

On the other hand, there are other departments I would like to thank for preventing the timely completion of this thesis. I have found physics and linguistics both distracting and stimulating as a mathematician. Somewhere between those disciplines, I now appreciate mathematics in a different light.

I am truely beholden to: Elchin Jafarov for being my first officemate and staying late every night, Dmitry Nicolsky for camaraderie and for being a fellow mycophile, Adlai Burman for cynical discourse and loving absurdism, Lyman Gillespie for enjoying beats and Snivlem, Jason Boyce for bus rides and bass lines, Shane Dayton for high literacy and telling good stories, Amy Keith for listening and gabbing over the years, Justin Yonker for much late-night pipe smoking philosophy and friendship, Safia Rawoot for feeding me and playing music, Carl Andersen for good bass lines and tasty beer, Mary Parsons for coffee and chitchat, Jimie Horath for a place to live, Jeff Martt for 'loaning' me his Pathfinder...

1 Delay Differential Equations

1.1 Background

Delay differential equations (DDE) are differential equations in which there is time lag. This corresponds to a nonzero amount of time between a signal and response, providing a system feedback timescale. Models of this form arise in applications in biology [32], engineering [31], ecology [30], chemistry [34], and other systems containing derivatives which depend on a previous states [18, 19, 25]. As with all such equations describing system dynamics, stability is a primary concern. One wants to determine whether the system collapses to a steady state or whether small inputs may grow large.

In this thesis, the class of investigated objects is restricted to linear problems.

Definition 1 *A linear DDE with a finitely many fixed delays is an equation*

$$\dot{y}(t) = A(t)y(t) + \sum_{k=1}^{n} B_k(t)y(t - \tau_k) \qquad (t, \tau_k \geq 0) \tag{1.1}$$

where $\tau_k > 0$ are positive scalar delays and $A(t), B_k(t)$ are time-dependent coefficients generally assumed to be at least piecewise continuous. The function $y(t)$ is the solution to such an equation.

Equation (1.1) is a linear DDE, although it may be intended to approximate the dynamics of a nonlinear system having the form

$$\dot{y}(t) = f(t, y(t), y(t - \tau_1), \ldots, y(t - \tau_n)) \qquad (t, \tau_k \geq 0). \tag{1.2}$$

In the case of a linear DDE with only one delay, coefficients $A(t)$ and $B(t)$

may be periodic in t. Of particular interest is the coincidence of the delay and the periodicity of these functions. In the single delay case when $A(t)$ and $B(t)$ are τ-periodic, Equation (1.1) simplifies to

$$\dot{y}(t) = A(t)y(t) + B(t)y(t - \tau) \qquad (t, \tau \geq 0) \qquad (1.3)$$

where $A(t+\tau) = A(t)$ and $B(t+\tau) = B(t)$. This is a linear DDE with coefficients equal in period to the delay and will be the primary focus of this discussion. When Equation (1.3) is written as $\dot{y}(t) = f(t, y(t), y(t - \tau))$, it is clear that value of $\dot{y}$ is determined by the three quantities t, $y(t)$, and $y(t - \tau)$. Note that $f(t, \cdot, \cdot) = f(t^*, \cdot, \cdot)$ when $t^* = t \mod \tau$. Applications of the linear case are found commonly as linearizations of nonlinear case where $f(t, y, \dot{y}) = f(t^*, y, \dot{y})$ [31, 15].

In order to have a well-posed problem, it is also necessary that a function $y(t)$ be specified on the interval $[-\tau, 0]$ by a function ϕ, $y(t) = \phi(t)$. This provides an initial condition which is an infinite set of values, making the DDE problem inherently infinite-dimensional. This continuum of values is frequently called a 'history function', and regularity of the DDE solutions are based in part on the regularity of the function ϕ. The following is proven in [4] and [18], for this case.

Theorem 1.1 *If $\phi \in C^0[-\tau, 0]$ is a given history function for the DDE of Equation (1.3) with $A(t), B(t) \in C^k[0, \tau]$, there is a unique function y satisfying (1.3) and $y(t) = \phi(t)$ for $t \in [-\tau, 0]$. There is increasing regularity of y over each period up to the regularity of the coefficients. Namely, $y \in C^n[(n - 1)\tau, n\tau]$ for $n = 0, 1, 2, \ldots, k + 1$, and $y \in C^{k+1}[(n - 1)\tau, n\tau]$ for $n > k + 1$.*

A direct corollary is that the eigenfunctions of Equation (1.3), those solutions y such that $y(t) = \lambda y(t - \tau)$ for some $\lambda \in \mathbb{C}$, are of class $C^\infty[-\tau, \infty)$

provided that $A(t), B(t) \in C^\infty[0, \tau]$. As a minimal requirement to construct a solution $y(t)$, the history function $\phi(t)$ need only be an element of $L^1[-\tau, 0]$ with $\phi(0)$ chosen; see Formula (1.7). Here, $L^1[a, b]$ is used to denote the set of scalar functions $\phi : [a, b] \to \mathbb{C}$ which are integrable in the Lebesgue sense.

1.2 Floquet Theory

Fundamental Matrix Solution

In the theory of ordinary differential equations (ODEs), a fundamental matrix solution to the linear ODE system

$$\dot{y}(t) = A(t)y(t) \qquad (y(t) : [t_0, \infty] \to \mathbb{C}^d, \ A(t) : [t_0, \infty] \to \mathbb{C}^{d \times d}) \qquad (1.4)$$

is a matrix-valued function $\Phi(t)$ which solves the system $\dot{\Phi}(t) = A(t)\Phi(t)$ with the condition that $\Phi(t_0)$ is invertible for some t_0 in an interval on which $A(t)$ is defined and integrable. The fundamental matrix solution can also be found as the solution of the integral equation

$$\Phi(t) = \Phi(t_0) + \int_{t_0}^{t} A(s)\Phi(s)ds$$

by integrating Equation (1.4) and applying the condition $\Phi(t_0) = I$. The matrix entries $\Phi_{ij}(t)$ are each continuous in time if $A(s)$ is integrable [13]. An important property of Φ is given in the next theorem whose complete proof is found in [13], and also gives a formal definition to the fundamental solution.

Theorem 1.2 *The time-dependent matrix $\Phi(t)$ is a fundamental solution to the homogeneous linear matrix ODE initial value problem*

$$\begin{cases} \dot{\Phi}(t) & = A(t)\Phi(t) \\ \det \Phi(t_0) & \neq 0 \end{cases}$$

if and only if the columns of $\Phi(t_0)$ are linearly independent. Also, Φ satisfies the equation

$$\det \Phi(t) = \Phi(t_0) \exp\left[\int_{t_0}^{t} \text{trace}\, A(s)\, ds\right]$$

which is known as 'Liouville's Formula'.

For any time t, the fundamental matrix solution has columns which are vector solutions of Equation (1.4), and span the solution space. Any function y solving $\dot{y} = A(t)y$ has a representation $y(t) = \Phi(t)c$ where entries of c are the coefficients of y written in the basis of columns of $\Phi(t)$. Note that the vector c is constant: the difference in the value of y at two different times is accounted for by the change in Φ.

First order ODE systems such as Equation (1.4) can have temporally periodic coefficients. Higher order systems with this property can also be reduced to a first order system with periodic coefficients, so the general d-dimensional ODE system with τ-periodic coefficients is given

$$\dot{y} = A(t)y, \qquad A(t+\tau) = A(t). \tag{1.5}$$

Note that such an ODE may have time-periodic coefficients but no nontrivial periodic solutions. A simple example is the evolution equation

$$\dot{y}(t) = (1 + \sin t)y(t)$$

whose coefficient is 2π-periodic. All classical solutions have the form $y(t) = ce^{t-\cos t}$, which are not periodic except for the trivial solution, $y = 0$.

Floquet's Theorem [28] describes some properties of these types of systems. In particular, it guarantees the existence of solutions satisfying a particular problem: an eigenvalue problem.

Theorem 1.3 *The d-dimensional ODE given in* (1.5) *with* $A(t) \in \mathbb{C}^{n \times n}$ *with period τ has at least one nontrivial solution $Y(t)$ so that $Y(t+\tau) = \mu Y(t)$. Such a function is called a* normal solution, *and $\mu \in \mathbb{C}$ is called a* characteristic multiplier.

Proof. If Φ is the fundamental matrix solution and A is periodic, $\Phi(t + \tau)$ is also a fundamental matrix solution as its determinant is non-vanishing by the previous theorem. Since columns of $\Phi(t)$ and $\Phi(t + \tau)$ span the same solution space, columns of $\Phi(t + \tau)$ are linear combinations of columns of $\Phi(t)$: $\Phi(t + \tau) = \Phi(t)K$ with K nonsingular. Let μ be an eigenvalue of K with associated eigenvector v. Then $Y(t) = \Phi(t)v$ is a solution of Equation (1.5). For this choice, $Y(t + \tau) = \Phi(t + \tau)v = \Phi(t)Kv = \Phi(t)\mu v = \mu Y(t)$. ∎

The complex values μ are also called *Floquet multipliers* in some literature. The previous theorem establishes that characteristic multipliers associated with a particular problem are independent of the choice of fundamental solutions.

The next theorem, whose proof may be found in [13], makes use of matrix exponentiation.

Definition 1.4 *The* matrix exponential *on $\mathbb{C}^{n \times n}$ is the map $X \mapsto e^X$ is defined by the Taylor series expansion*

$$e^X = \exp(X) = I + \sum_{k=1}^{\infty} \frac{X^k}{k!}$$

where I is the identity of the appropriate space.

Theorem 1.5 *If $\Phi(t)$ is the fundamental solution to the ODE of Equation* (1.5), *then*

$$\Phi(t + \tau) = \Phi(t)\Phi^{-1}(0)\Phi(\tau)$$

for all $t \in \mathbb{R}$. Also, there exists $C \in \mathbb{C}^{n \times n}$ such that $\exp(C\tau) = \Phi^{-1}(0)\Phi(\tau)$, and there is a τ-periodic complex matrix function $P(t)$ such that $\Phi(t) = P(t)\exp(Ct)$ for each $t \in \mathbb{R}$.

The representation of the fundamental solution as $P(t)\exp(tC)$ is called the *Floquet normal form*. The *Floquet transition matrix*

$$\Phi(\tau)\Phi^{-1}(0),$$

which is independent of t, is the map which takes a vector v and moves it forward in time by an amount τ [13]. It does so by keeping track of changes in which the basis v is represented, allowing for information to be translated from one state to a single period later. A useful theorem, also appearing in [13], is relevant to the discussion of different approaches to analyzing the stability of solutions to Equation (1.5).

Theorem 1.6 *If λ is a characteristic multiplier of the linear τ-periodic differential equation* (1.5) *and $\exp(\mu\tau) = \lambda$, then there is a solution of the form*

$$x(t) = p(t)e^{\mu t}$$

where p is τ-periodic and $x(t + \tau) = \lambda x(t)$.

In the constant coefficient case, τ can be chosen to be any positive number when applying the theorem, giving a relationship between the eigenvalues of the infinitesimal generator of an evolution semigroup and eigenvalues of a discrete time operator, discussed later in this section.

1.3 Monodromy Solution of DDEs

The Method of Steps

Floquet Theory is a language formulated for periodic ODEs. When the coefficients $A(t), B(t) \in \mathbb{C}^{d \times d}$ of the DDE (1.3) have entries which are τ-periodic, there is a special formulation of its solution in this language. While results of Floquet Theory are not immediately extensible to DDEs, it does provide an analogue of the more complicated dimensional situation for DDEs [21]. In order to solve DDEs, an operator can be used in order to 'time advance' the data of a previous solution at time $t - \tau$ to the current time t. In this manner, Equation (1.3) can be solved iteratively over intervals of length τ. That is, the DDE problem can be solved by applying a linear operator $\mathcal{U}$ to the history function $\phi(t)$ defined on $[-\tau, 0]$, generating solution on the next interval:

$$\begin{aligned}
Y_0(t) &= \phi(t) & (t \in [-\tau, 0]) \\
Y_n(t) &= \mathcal{U}Y_{n-1}(t) & (t \in [(n-1)\tau, n\tau], n = 1, 2, \ldots).
\end{aligned} \tag{1.6}$$

The process of finding a solution in the manner of equation (1.6) is known as the 'method of steps'. A solution is found on the interval $[n\tau, (n+1)\tau]$ based on a previous solution over $[(n-1)\tau, n\tau]$. Since the coefficients of the DDE are τ-periodic, it is possible to regard the delayed part of the DDE, represented by $B(t)y(t - \tau)$, as an inhomogeneity and apply a variation of parameter method to find the solution at this later time.

It is not necessary that the history function be continuous, especially at the initial point. That is, it is not at all necessary to have $y(0) = \phi(0)$, only that $\phi(0)$ be defined. Otherwise, input function ϕ needs only to be integrable for a variation of parameter technique to be applied.

Theorem 1.7 *A solution, y, to the system* (1.3) *at time* $t \in [0, \tau]$ *assuming*

$\phi \in \mathbb{C}^d \oplus \left(\mathbb{C}^d \otimes L^1[-\tau, 0]\right)$ *and* $\phi(0) \in \mathbb{C}^d$ *are defined is given by*

$$y(t) = \Phi(t) \left[\phi(0) + \int_0^t \Phi^{-1}(s)B(s)\phi(s-\tau)ds\right], \quad t \in [0, \tau] \qquad (1.7)$$

where $\Phi(t)$ *is a fundamental solution of* $\dot{y}(t) = A(t)y(t)$.

Definition 1.8 *The operator* $\mathcal{U}_0$, *called the* monodromy operator *associated with the DDE* (1.3), *is defined as the operation on* ϕ *to produce* y *in Equation* (1.7).

The monodromy operator could also be called the 'Delayed Floquet Transition Operator associated with the DDE (1.3).' The 'Floquet' part of the nomenclature is justified by the description of fixed information propagating periodically through the system. However, in ODE theory, there is a finite dimensional Floquet transition matrix. The periodic coefficient DDE analogue of the theory has an infinite dimensional operator.

Some behavior of solutions and properties of the solution operator can be found by investigating the terms in Equation (1.7).

$$(\mathcal{U}_0\phi)(t) = \underbrace{\Phi(t)\phi(0)}_{\text{Undelayed}} + \underbrace{\Phi(t) \int_0^t \Phi^{-1}(s)B(s)\phi(s-\tau)ds}_{\text{Delayed}} \qquad (1.8)$$

The undelayed part is simply the fundamental solution applied to the endpoint of the initial data. It solves the ODE $\dot{y} = Ay$ with $y(0) = \Phi(0)\phi(0) = \phi(0)$. The delayed part of the solution operator requires further consideration.

The delayed part can be decomposed into parts. First, the expression $B(s)\phi(s-\tau)$ is self explanatory; it is the delay coefficient evaluated at time s applied to the initial data from time $s-\tau$. Then the inverse of the fundamental solution , Φ^{-1}, is applied, rewriting $B(s)\phi(s-\tau)$ in the basis of the fundamental solution at time s. This "shifts time backward" to the beginning of the interval

$[0, \tau]$ so that previous values of the data function can be used. Since they are written in the basis of the fundamental matrix solution, they are a solution of the DDE at those times. This quantity is then integrated from $s = 0$ to $s = t$ so that the effects of the history function for times $-\tau$ to $t - \tau$ are accounted for. Finally, the application of $\Phi(t)$ rewrites this in the basis appropriate for having solved the DDE on the time interval 0 to t. In sum, the delayed part of Equation (1.8) adds up the delayed coefficient matrix applied to the solution over times within the previous period, written in the basis of the fundamental solution at those times. This cumulative effect is finally multiplied against $\Phi(t)$ to produce a particular solution.

Once the monodromy operator is found, solutions to the DDE system

$$
\begin{aligned}
\dot{y}(t) &= A(t)y(t) + B(t)y(t - \tau) \quad (t > 0) \\
y(t) &= \phi(t - \tau) \quad\quad\quad\quad\quad (-\tau \le t \le 0)
\end{aligned}
\tag{1.9}
$$

with $A(t + \tau) = A(t)$ and $B(t + \tau) = B(t)$ can be found by the method of steps. This is done by applying the monodromy operator iteratively to a history function $\phi : [-\tau, 0] \to \mathbb{C}$ which generates a solution $\mathcal{U}_0 \phi : [0, \tau] \to \mathbb{C}$.

$$
y(t) = (\mathcal{U}_0^k \phi)(t - k\tau) \text{ where } t \in [0, \infty), \text{ and } k = \lfloor t/\tau \rfloor.
\tag{1.10}
$$

The right space

In order to investigate some properties of the monodromy operator $\mathcal{U}_0$, it will need to be recast into a Hilbert space operator whose domain and range spaces are identical. This is motivated by the desire to have eigenvalues and an inner-product, discussed later in Section 3.3. In Definition 1.8, monodromy operator maps the space $\mathbb{C} \oplus L^1[0, \tau]$ to the space of absolutely continuous functions on $[0, \tau]$. That is, $\mathcal{U}_0 : \mathbb{C} \oplus L^1[0, \tau] \to C[0, \tau]$. Note that continuity no longer requires the specification of an initial point.

Since $L^1[0,\tau]$ contains $L^2[0,\tau]$, the domain of $\mathcal{U}_0$ can be restricted to the Hilbert space $\mathcal{H} := \mathbb{C} \oplus L^2[0,\tau]$ and remain a bounded operator [7]. The elements $\phi \in C[0,\tau]$ can be associated isomorphically associated with pairs $(\phi(0), \phi) \in \mathbb{C} \oplus C[0,\tau]$. Since $C[0,\tau]$ is dense in $L^2[0,\tau]$, the range of $\mathcal{U}_0$ can be extended to $\mathcal{H}$ again preserving its boundedness. The monodromy operator, denoted simply by $\mathcal{U}$ hereafter, will act from the Hilbert space $\mathbb{C} \oplus L^2[0,\tau]$ to itself, and its eigenvalues will be well defined.

Theorem 1.9 *The monodromy operator* $\mathcal{U} : \mathbb{C} \oplus L^2[0,\tau] \to \mathbb{C} \oplus L^2[0,\tau]$ *is a compact bounded linear operator.*

Proof. Linearity is verified by noting for two elements of the input space

$$(\phi(0), \phi), (\psi(0), \psi) \in \mathbb{C} \oplus L^2([0,\tau]),$$

one has

$$
\begin{aligned}
\mathcal{U}((\phi(0), \phi) + (\psi(0), \psi)) &= \mathcal{U}(\phi(0) + \psi(0), \phi + \psi) \\
&= \Phi(t) \left(\phi(0) + \psi(0) + \int_0^t \Phi^{-1}(s) B(s)(\phi + \psi)(s - \tau) \, ds \right) \\
&= \Phi(t) \left(\phi(0) + \int_0^t \Phi^{-1}(s) B(s)\phi(s - \tau) \, ds \right. \\
&\quad \left. + \psi(0) + \int_0^t \Phi^{-1}(s) B(s)\psi(s - \tau) \, ds \right) \\
&= \mathcal{U}(\phi(0), \phi) + \mathcal{U}(\psi(0), \psi).
\end{aligned}
$$

Let $(\phi(0), \phi)$ be an element of $\mathbb{C} \oplus L^2[0,\tau]$. Define

$$f(t) = \int_0^t \Phi^{-1}(s) B(s)\phi(s - \tau) \, ds$$

and note that f is absolutely continuous as it is an indefinite integral. The

natural norm for $f \in C[0, \tau]$ is the supremum norm, so that

$$
\begin{aligned}
\|f\|_\infty &= \operatorname*{ess\,sup}_{t \in [0,\tau]} \left| \int_0^t \Phi^{-1}(s) B(s) \phi(s - \tau) ds \right| \\
&\leq \operatorname*{ess\,sup}_{t \in [0,\tau]} \int_0^t \left| \Phi^{-1}(s) B(s) \phi(s - \tau) \right| ds \\
&\leq \operatorname*{ess\,sup}_{t \in [0,\tau]} \left\| \Phi^{-1} B \right\|_{L^2[0,t]} \|\phi\|_{L^2[0,t]} \\
&\leq \left\| \Phi^{-1} \right\|_\infty \|B\|_\infty \|\phi\|_2 = C_B \|\phi\|_2
\end{aligned}
$$

for some finite constant C_B which depends on the coefficient B and fundamental matrix solution Φ. This demonstrates that $\|f\|_\infty$ is bounded with respect to $\|\phi\|_2$. Note that Φ is invertible, so $\|\Phi^{-1}\|_\infty$ is finite. Also, $B(t)$ is a bounded matrix defined over a closed finite interval, so $\|B\|_\infty$ is also finite.

Over a domain of finite measure, as is the interval $[0, \tau]$, the supremum norm dominates the 2-norm [35]. Then for some $C > 0$,

$$
\begin{aligned}
\|\mathcal{U}\phi\|_2 \leq C \|\mathcal{U}\phi\|_\infty &= C \left\| \Phi(t) \left(\phi(0) + \int_0^t \Phi^{-1}(s) B(s) \phi(s - \tau) \, ds \right) \right\|_\infty \\
&\leq C \|\Phi\|_\infty \left(|\phi(0)| + \|f\|_\infty \right) \leq C \|\Phi\|_\infty \left(|\phi(0)| + C_B \|\phi\|_2 \right) \\
&\leq C \|\Phi\|_\infty \left(1 + C_B \right) \|\phi\|_2
\end{aligned}
$$

which shows that $\mathcal{U}$ is bounded provided $\phi(0) \in \mathbb{C}$ is finite. Proof of compactness of $\mathcal{U}$ is found in [8, 21], which apply to $\mathcal{U}$ results found in [26]. ∎

Operators which are compact can be regarded as limits of finite rank operators or matrices. Consequently, the spectrum of the compact operator $\mathcal{U}$ consists only of eigenvalues, except possibly for $0 \in \mathbb{C}$. Further, it is expected that the eigenvalues of matrix approximations to $\mathcal{U}$ will converge to the spectrum of $\mathcal{U}$.

Compact operators have another important property: the origin is the only

possible cluster point of eigenvalues, and may be the only spectral element which is not an eigenvalue. Matrix approximations of operators can be expected to converge in spectrum to the eigenvalues of the operator, beginning with those of greatest modulus [39, 38]. That is, the 'shape' of a compact operator is associated with the eigenvalues of largest modulus, and a good approximation should get the 'shape' correct quickly, with a low rank approximation. Improving the approximation with matrices of higher rank fills in 'details' by getting smaller eigenvalues correct.

1.4 Stability Analysis of DDEs

Stability analysis of nonlinear equations is important in many fields of science. Many technical tools for doing such analysis first require appropriate linearizations. A general nonlinear delay system with one delay $\dot{y}(t) = f(t, y(t), y(t - \tau))$ can be linearized about a periodic solution $y(t)$, for example, to give linear DDE such as (1.3)

For practical applications, it is natural to ask whether the zero solution of a homogeneous linear DDE with periodic coefficients is stable. Asymptotic stability of an DDE means that for each y solving the DDE, $y(t)$ vanishes in the limit as $t \to \infty$. The question is usually dependent on choices of parameters appearing in the DDE such as the coefficients $A(t)$ and $B(t)$ as well as the duration of delay. The focus here is on coefficients; the delay, τ, is assumed to be fixed.

The stability of a DDE may be discerned through an investigation of the spectrum of $\mathcal{U}$, the monodromy operator. As noted above, the eigenvalues of $\mathcal{U}$ are analogous to the Floquet multipliers for a periodic ODE. Floquet multipliers being less than unit magnitude implies that a solution must be damped eventually. Equivalently, the eigenvalues of the monodromy operator being within the unit disc of $\mathbb{C}$ ensure that all solutions vanish in the limit.

The set of DDE multipliers comprise the point spectrum of $\mathcal{U}$, which is well approximated by matrices under appropriate hypotheses [8]. If the approximation to $\mathcal{U}$ is implemented spectrally or in some other 'good' way which converges rapidly to $\mathcal{U}$, then the largest modulus eigenvalues of the approximation are good approximations to the eigenvalues of $\mathcal{U}$, and hence to the multipliers.

Iterative Time Processes

Equations (1.6) and (1.10) reveal something important about the method of steps. They characterize this method of finding a solution over time intervals of a fixed-length time interval as an iterative process. Formally, stability criterion for iteration is given in the following theorem with proof given in [22]. Recall that for an operator $\mathcal{A} : X \to Y$ where X and Y are spaces with norms $\|\cdot\|_X$ and $\|\cdot\|_Y$, respectively, the operator norm is given by

$$\|\mathcal{A}\| = \sup_{x \in X} \frac{\|\mathcal{A}x\|_Y}{\|x\|_X}.$$

Theorem 1.10 *For an operator $\mathcal{A}$ (or matrix $A \in \mathbb{C}^{n \times n}$), in order that $\|\mathcal{A}^k\| = 0$ in the limit as $k \to \infty$, it is necessary and sufficient that the largest eigenvalue of A have modulus less than unity [22]. Such an iterative process is said to be Schur stable [3].*

This asymptotic stability criterion requires that the eigenvalues of the monodromy operator lie in the interior of the unit circle. Knowing the asymptotic stability does not give a bound on the behavior of $\mathcal{U}$ in finite time; it only says that for any input, the solution of a DDE is eventually damped out.

Continuous Time Processes

There exist other approaches to analyzing the stability of DDEs, as there are other methods for solving them. One of note is a semigroup formulation, found in [1]. This formulation of the original DDE as an evolution equation, called an abstract Cauchy problem in most literature, is a standard process for proving regularity results [1, 2]. However, this approach is applicable only to constant coefficient DDEs such as $\dot{y}(t) = Ay(t) + By(t-\tau)$. The Cauchy problem associated with this equation is $\dot{Y}(t) = \mathcal{A}Y(t)$, solved by $Y(t) = Y(0)e^{\mathcal{A}t}$. Here, the initial data of the history function is encoded into $Y(0)$.

The operator $\mathcal{A}$ is the infinitesimal generator of a 'delay semigroup' [1], and its eigenvalues are related to the eigenvalues of the monodromy operator by Theorem 1.6. In this approach, unlike the monodromy approach, the time axis is not divided into intervals of fixed length and the process cannot be represented by operator or matrix iteration. Instead, the formulation is for continuous time and requires a different approach to stability analysis. A proof of the following theorem for the matrix case is available in [5]. The *spectral abscissa*, $\alpha(\mathcal{A})$, maximum real part of the eigenvalues of $\mathcal{A}$.

Theorem 1.11 *Let $\mathcal{A}$ be an operator or matrix in $\mathbb{C}^{n \times n}$ which corresponds to a process under continuous time. In order that $\lim_{t \to \infty} \left\| e^{t\mathcal{A}} \right\| = 0$, it is necessary and sufficient that $\alpha(\mathcal{A})$ be negative. Such a process is called* Hurwitz *stable*.

In a continuous application process, it is the spectral abscissa which determines the asymptotic limit of the matrix or operator which generates the process. Imaginary parts of eigenvalues contribute to oscillation while real parts correspond to growth or decay. Stability requires simply that all eigenvalues correspond to decay, with or without oscillation. This means a stable process will have all eigenvalues of the generator in the left half plane of $\mathbb{C}$.

In the case of DDEs with constant coefficients, there is a purely algebraic method of analyzing stability via the Laplace transform, $\mathcal{L}$ [25]. Suppose y is a solution to equation $\dot{y}(t) = Ay(t) + By(t - \tau)$ with $y(0) = 0$ and $A, B \in \mathbb{C}^{n \times n}$. Let $Y(s) = [\mathcal{L}y](t)$. Then $sY(s) = AY(s) + Be^{-\tau s}Y(s)$ or $(sI - A - Be^{-\tau s})Y(s) = 0$ or

$$sI - A - Be^{-\tau s} = 0 \tag{1.11}$$

for nontrivial Y. This is known to be stable if and only if the values of s which satisfy Equation (1.11) are in the open left half of the complex plane [23]. Figure 1.1 graphically illustrates Schur and Hurwitz views of analyzing stability.
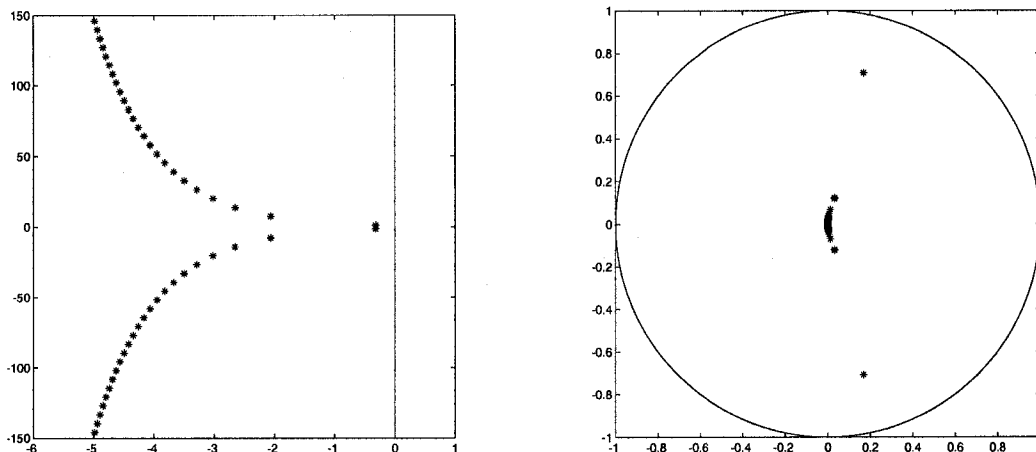
Figure 1.1 Two Perspectives on Stability: Hurwitz and Schur. Two different perspectives of stability for the DDE $\dot{y}(t) = -y(t - 1)$. On the left are roots of Equation (1.11), with the imaginary axis shown. On the right are eigenvalues of an approximation to the monodromy operator with the unit circle shown. Both reveal the stability of the DDE with Hurwitz criterion applied to the former and Schur criterion to the latter.

Stability Charts

Often, DDEs depend on parameters. When this is true, it is useful to know which choices of parameter lead cause the equation to be stable in the senses discussed above. One method is to numerically generate a grid within the parameter space and determine whether the DDE is stable for each set of parameters in the grid. The result is a *stability chart* of the parameter space where, for example, dark regions represent parameter choices leading to instability, and light regions represent those for which the DDE is stable. An example chart for a constant coefficient scalar DDE is given in Figure 1.2.

DDECSPECT stability chart. m = 13 Cheb colloc pts.
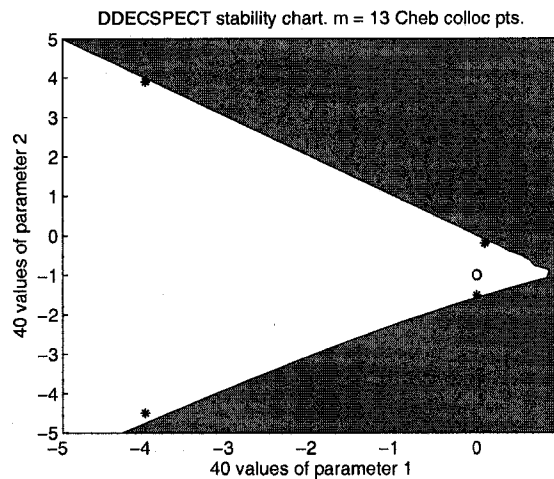
Figure 1.2 A Stability Chart for Scalar Linear DDEs. The a 2-dimensional stability chart for the constant coefficient DDE $\dot{y}(t) = ay(t) + by(t-1)$. Here, the parameters are the coefficients. The points identified with asterisks are $(1, -.2)$, $(-4, 3.9)$, $(-4, -4.5)$ and $(0, -1.5)$ are all within the stability region. Circled is the point $(0, -1)$, showing that Figure 1.1 illustrates eigenvalues which go with a point in the stable region of parameter space.

2 Normality

The spectral theorem for self-adjoint (symmetric or hermitian) matrices states that there exists an orthonormal basis (ONB) for matrix $A \in \mathbb{C}^{n \times n}$ so that A can be represented by a diagonal matrix $\Lambda \in \mathbb{C}^{n \times n}$ whose entries are the eigenvalues of A. This means that a self-adjoint matrix is diagonalized in a basis of its eigenvectors, which is possible since the eigenvectors are orthogonal. The class of normal matrices generalizes the hermitian case. Here, it is not necessary that a matrix and its adjoint be coincident, but need only commute with one another.

Definition 2.1 *A matrix A is* normal *whenever $A^*A = AA^*$ where $(A^*)_{jk} = \overline{A}_{jk}$.*

Theorem 2.2 *[40] For a matrix $A \in \mathbb{C}^{n \times n}$, the following are equivalent:*

1. *A is normal.*

2. *A has a complete set of orthogonal eigenvectors.*

3. *A is unitarily diagonalizable.*

Each of the items in this theorem is dependent on a choice of inner product. For item 1, this is implicit as the adjoint space is formally defined though inner products. Dependence of the second item is clear by recalling that two vectors are orthogonal when their inner product vanishes. Finally, item 3 refers to unitary objects, those matrices Q for which $Q^* = Q^{-1}$. Again, the dependence is implicit as in item 1 since this is equivalent to $\langle Qx|y \rangle = \langle x|Q^{-1}y \rangle$ for all x and y in the inner product space on which Q acts. In particular, only matrices (and operators) acting on inner product spaces can be specified as 'normal' or 'not normal' [37].

Unitary diagonalization is a very special property. Geometrically, it means that it is only necessary to rotate or reflect the standard basis axes of $\mathbb{C}^{n \times n}$ to align with the eigenvectors of A.

An argument for the following is found in [40].

Corollary 2.3 *The class of normal matrices includes self-adjoint, unitary, and skew-hermitian matrices.*

2.1 Measuring Non-Normality

Abstractly, a matrix is the representation of an operator on a finite dimensional space in a particular basis. This basis may be changed through similarity transformation which leave the eigenvalues unchanged. The change of basis is reflected in the eigenvectors, however.

Theorem 2.4 *For a matrix $A \in \mathbb{C}^{n \times n}$ and non-singular $S \in \mathbb{C}^{n \times n}$, the set of eigenvalues of A is invariant under the similarity transformation induced by S. That is,*

$$\Lambda(A) = \Lambda(SAS^{-1})$$

where $\Lambda(X)$ denotes the set of eigenvalues of a matrix X. Moreover, if v_k is an eigenvector of A associated with $\lambda_k \in \Lambda(A)$, Sv_i is an eigenvector of SAS^{-1} associated with λ_k.

Proof. Note that the requirement that S be non-singular means that S^{-1} exists and is unique. If A is diagonalizable, $A = V\Lambda V^{-1}$ where Λ is a diagonal matrix whose elements are the eigenvalues of A. Applying S, $SAS^{-1} = (SV)\Lambda(SV)^{-1}$ is a diagonalization of SAS^{-1}, which has the same diagonal matrix, Λ, of eigenvalues as A. Hence $\Lambda(A) = \Lambda(SAS^{-1})$. Suppose $\lambda \in \Lambda(A)$ with associated eigenvector v, so that $Av = \lambda v$. Take $w = Sv$. Then $SAS^{-1}w = SAS^{-1}Sv = SAv = \lambda Sv = \lambda w$ so Sv is the eigenvector of SAS^{-1} associated

with $\lambda \in \Lambda(SAS^{-1})$. In the case that A is not diagonalizable, a more general proof using the Jordan form of A is provided in [22]. ∎

For a normal matrix $A \in \mathbb{C}^{n \times n}$, there is a unitary similarity transformation V so that VAV^{-1} is diagonal. On the other hand, matrices are typically diagonalizable. A matrix is diagonalizable if and only if it is non-defective [39], that is, if the algebraic multiplicity of each of its eigenvalues equals the geometric multiplicity its eigenvalues. Normal matrices have the distinguishing property of being *unitarily* diagonalized. The remainder of this work assumes implicitly that subject matrices are diagonalizable.

For matrices which are not normal, it is useful to know just how 'efficient' a basis is for modeling a particular process. In the case of matrices which are not normal, analysis requires a more quantitative assessment. There are several methods of quantifying both the property of normality and measuring how far a matrix deviates from it, and different measures provide different insights. An example of the disparity between common measures is provided in [20] and in section seven of [37]. Here, the discussion focuses on measures based on eigenvector conditioning, Henrici departure, numerical range, and finally, resolvents and ε-pseudospectra.

Eigenvector Conditioning

In light of item 2 in Theorem 2.2, there is a way of characterizing and defining normality of a matrix A through the inner product of its eigenvectors. The definition is similar for linear operators on a Hilbert space. For the next definition, recall that for $B \in \mathbb{C}^{m \times n}$, the 2-norm of B is defined as

$$\|B\|_2 = \max_{\substack{x \in \mathbb{C}^n \\ x \neq 0}} \frac{\|Bx\|_2}{\|x\|_2} = \max_{\substack{x \in \mathbb{C}^n \\ x \neq 0}} \sqrt{\frac{(Bx)^*Bx}{x^*x}}.$$

where $\|x\|_2$ denotes the vector 2-norm of $\mathbb{C}^n$ and $x^*x = \sum_{j=1}^n |x_j|^2$ is the inner product.

Definition 2.5 *The* 2-*norm* condition number *of an invertible matrix* $V \in \mathbb{C}^{n \times n}$ *is defined as* $\kappa(V) = \|V\|_2 \|V^{-1}\|_2$.

For a matrix $A \in \mathbb{C}^{n \times n}$, the *eigenvector matrix condition number* of A is the condition number of the eigenvector matrix V. If $\{v_j\}_{j=1}^n$ are *normalized* eigenvectors of A, then $V = [v_1|v_2|\cdots|v_n]$. The number $\kappa(V)$ is a scalar value corresponding to how far from orthogonal the eigenvectors of A are in total.

Other equivalent ways of arriving at the condition number of the eigenvector matrix of A exist, as there are other structure-revealing factorizations of A other than diagonalization. Prevalent among these tools, especially as a numerically stable method for solving various problems, is the singular value decomposition (SVD). Here, a matrix A is written as the product of three matrices.

Theorem 2.6 *Every matrix* $A \in \mathbb{C}^{m \times n}$ *has a* SVD *where* $A = U\Sigma V^*$. *Here* $U \in \mathbb{C}^{m \times m}$ *and* $V \in \mathbb{C}^{n \times n}$ *are unitary matrices whose columns are called* right *and* left *singular vectors of* A, *respectively. The middle matrix* $\Sigma \in \mathbb{C}^{m \times n}$ *has only nonzero entries* $\Sigma_{jj} = \sigma_j \geq 0$, *which are ordered decreasingly and called* singular values *of* A.

Proof. A complete proof and definitions, as well as the geometric interpretation is provided in chapters four and five of [39]. ∎

A second definition for the condition number of the eigenvector matrix of A is provided by the singular values. These singular values σ_i are the positive square roots of the eigenvalues of AA^* or A^*A. The following definition is given in [40].

Definition 2.7 *If V is the eigenvector matrix of $A \in \mathbb{C}^{n \times n}$ where $\{\sigma_j\}_1^n$ are the singular values of V, the 2-norm eigenvector matrix condition number of A is*

$$\kappa(V) = \frac{\sigma_{\max}}{\sigma_{\min}} = \frac{\sigma_1}{\sigma_n}.$$

Note that this definition of $\kappa(V)$ is product of the largest singular values of V^{-1} and V. Note that when V is unitary, Σ is the identity. When V is unitary, both V and its inverse have norm 1, and hence $\kappa(V) = 1$. If $\kappa(V) = 1$, then V has $\sigma_{\max} = \sigma_{\min}$. As columns of V are normalized, both these values must be 1, so V is unitary. An immediate consequence of item 3 of Theorem 2.2 is given in the following corollary.

Corollary 2.8 *[39] A matrix A is unitarily diagonalizable if and only if it has eigenvector matrix V with $\kappa(V) = 1$. Thus, an appropriate addition to the list of theorem 2.2 is*

4. There is a diagonalization $A = V \Lambda V^{-1}$ for which $\kappa(V) = 1$.

The condition number of V then represents a measure of how far from unitary V must be to diagonalize A. If $\kappa(V)$ is 'large' for the best choice of V, A is said to be strongly non-normal. Such matrices are a practical concern, for if a matrix $A = V \Lambda V^{-1}$ where $\kappa(V)$ is large, use of this diagonalization may decrease numerical stability of the problem one wishes to solve. This is to say that the eigenvalues may not be useful since the eigenvector basis is, in some sense, a bad way to represent the matrix [39].

Other Measures

Another measure for the non-normality of a matrix A can be derived by assessing the total size of the off-diagonal entries when an optimal unitary transformation is applied to A. Such an approach leads to a quantity called

Henrici's departure from normality. It is found using the Schur factorization of A, which is guaranteed to exist whenever $A \in \mathbb{C}^{n \times n}$ [39], although it may not be unique. First, factor $A = QTQ^*$ where Q is unitary and T is upper-triangular. Then assign a scalar value defined as the Frobenius norm of the matrix T with the diagonal entries removed [22]. This number is unique, entries of T are unique up to signs. The Frobenius norm of $X \in \mathbb{C}^{m \times n}$ is defined as

$$\|X\|_F = \left(\sum_{j=1}^{n} \|x_j\|_2^2 \right)^{1/2} = \left(\sum_{j,k=1}^{n} |x_{jk}|^2 \right)^{1/2}$$

where x_j are the m columns of X.

Definition 2.9 *For $A \in \mathbb{C}^{n \times n}$, the* Henrici departure *is the number*

$$D_H = \|T - diag(T)\|_F$$

where $A = QTQ^*$ is a Schur factorization of A and $diag(T)_{jk} = \delta_{jk}T_{jk}$.

For the complex Schur factorization, the main diagonal entries are the eigenvalues. The complex Schur factorization of any normal matrix is simply its unitary diagonalization. Generally, the total sum of squares of the off-diagonal entries of T then provides a meaningful measure of how far this 'best' unitary transformation fails to diagonalize A [20]. Note that the complex Schur factorization is distinct from the real Schur factorization.

Another measure goes by the names 'numerical range', or 'field of values'. This can be thought of as the set of all values obtained from taking inner products of elements of the unit disc of $\mathbb{C}^n$ with themselves under weight A. The set is formally given by $W(A) = \{\langle x|Ax \rangle = x^*Ax \mid \|x\| = 1\}$ and is a convex region of the complex plane. Note that $W(A) \supset \Lambda(A)$, regardless of the structure of A. The shape of $W(A)$ and its relation to $\Lambda(A)$ can be used to discern facts about the behavior of A.

There is a simple characterization of $W(A)$ in some cases: $A = A^*$ if and only if $W(A) \subset \mathbb{R}$ [24]. The matrix A is hermitian positive-definite if and only if $W(A) \subset \mathbb{R}^+$. For general matrices, there is no such particularly nice fact. However, some facts about the normality can be assessed by studying the numerical range. For example, when $W(A)$ is a line segment in $\mathbb{C}$, A is normal, but not conversely. The extrema of $W(A)$, in the sense of modulus, provide information about $\Lambda(A)$: they are moduli of the largest and smallest eigenvalues of A. Unitary matrices thus have $W(A) \subseteq \partial \mathbb{D}$. Note that $\mathbb{D}$ is used here to denote the open unit disc; generally, the notation $\mathbb{D}_r$ will be used to denote the set of points in the plane with modulus less than r. Perturbations of A induce changes in $W(A)$ which may used to measure the non-normality [24].

2.2 Resolvents

An oft used tool in the spectral analysis of matrices and operators is the resolvent.

Definition 2.10 *For a matrix $A \in \mathbb{C}^{n \times n}$ with a set of eigenvalues $\Lambda(A)$, the matrix valued function $\mathcal{R}_A : \mathbb{C} \backslash \Lambda(A) \to \mathbb{C}^{n \times n}$ defined as*

$$\mathcal{R}_A(z) = (zI - A)^{-1}$$

is called the resolvent *where I is the identity of $C^{n \times n}$.*

Note that $\Lambda(A)$ is excluded from the domain of $\mathcal{R}_A$ since $(zI - A)$ is singular for $z \in \Lambda(A)$, and hence is not invertible. For each sequence $z_i \in \mathbb{C} \backslash \Lambda(A)$ which converges to an eigenvalue λ of A, the norm of the resolvent becomes unbounded as $z_i \to \lambda$. The resolvent has been used to develop numerous different bounds on the spectrum of operators and matrices; many results and analysis in classical texts such as [29] are obtained through this approach.

Analysis of the resolvent norm function

$$f_A(z) := \|\mathcal{R}_A(z)\| = \|(zI - A)^{-1}\| \tag{2.1}$$

for $z \in \mathbb{C}$ reveals important nuances of the structure of the spectrum of A. This map transforms spectral information about an operator or matrix to the structure of f_A over complex plane. Spectral analysis results are obtained from bounds on the function f_A, which is bounded on compact subsets of $\mathbb{C}\backslash\Lambda(A)$. Much of the literature on spectral properties of operators on Hilbert spaces uses complex analysis techniques (cf. [29, 16]). The poles, $\{\lambda\}$ of f_A are the eigenvalues of A, and the rates at which sequences $\{z_i\} \to \lambda$ diverge give additional information about the behavior of $\mathcal{R}_A$ at points near $\Lambda(A)$.

In the case where A is normal, the reciprocal of the function f_A has a useful geometric interpretation. It is a ' reciprocal distance to spectrum' function, with $f_A(z) = \text{dist}(z, \Lambda(A))^{-1}$, where $\infty^{-1} := 0$. Note that for a set $X \subset \mathbb{C}$, $\text{dist}(z, X) = \inf_{x \in X} \text{dist}(z, x)$.

Proposition 2.11 *If $D \in \mathbb{C}^{n \times n}$ is a diagonal matrix and I is the identity of the appropriate space, $\|(zI - D)^{-1}\| = \text{dist}(z, \Lambda(D))^{-1}$.*

Proof. Since D is diagonal, the eigenvalues of D are found along the diagonal, so $D_{kk} = \lambda_k$. For $z \in \mathbb{C}$, $\Lambda(zI - D)^{-1} = \{z - \lambda_k\}$. The norm of a diagonal matrix is its spectral radius. Since $(zI - D)^{-1}$ is diagonal,

$$\|(zI - D)^{-1}\| = \max_{1 \leq k \leq n} \left| \frac{1}{z - \lambda_k} \right| = \frac{1}{\min_{1 \leq k \leq n} |z - \lambda_k|} = \frac{1}{\text{dist}(z, \Lambda(D))}.$$

If $z \in \Lambda(D)$, then $z - \lambda_k = 0$ for some k, so $1/(z - \lambda_k) = \infty$ by convention. That $\|(zI - D)^{-1}\| \geq (z - \lambda_k)^{-1}$ then implies $\|(zI - D)^{-1}\| = \infty$. ∎

The inverse distance, however, only serves as a lower bound on the distance in the general case where A is not normal or diagonal, as illustrated

in Figure 2.1. Note that the metric used to define distance induces the norm used in the definition of f_A [40]; the 2-norm taken for f_A implies Euclidean distance in $\mathbb{C}$, and also relates to the 2-norm condition number of the next proposition.
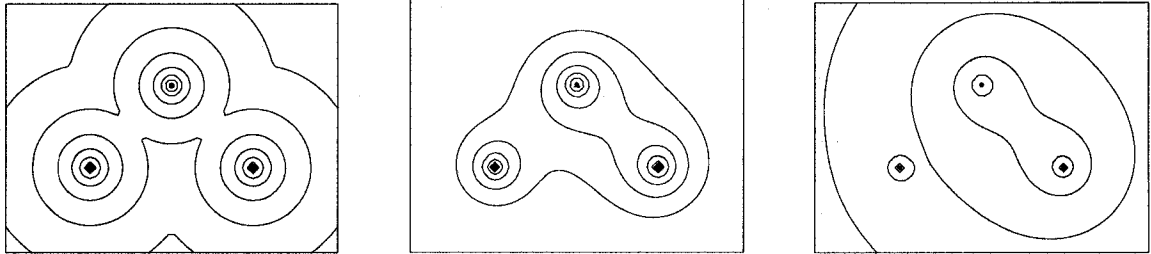

Figure 2.1 The Resolvent Norm Contours of Non-normal Matrices. The figures above show level curves for $10^{-1}, 10^{-1.25}, \ldots$ of the reciprocal of 2-norm resolvent, although the outermost curves are not visible in the rightmost plots. The matrices are similar, and hence have the same eigenvalues. The matrices have increasingly ill-conditioned eigenvector matrices with $\kappa(V) = 1,\ 3.78,\ 21.6$ (left to right).

Proposition 2.12 *Let A be a diagonalizable matrix or operator and I be the identity on the appropriate space. Then for all $z \in \mathbb{C}$,*

$$\left\| (zI - A)^{-1} \right\|_2 \geq \mathrm{dist}(z, \Lambda(A))^{-1}$$

with equality for all $z \in \mathbb{C}$ if and only if A is normal.

Proof. Since A is diagonalizable, there exists a similarity transformation $A = V\Lambda V^{-1}$ where Λ is diagonal and whose entries consist of eigenvalues of A. Then $(zI - A) = V(zI - \Lambda)V^{-1}$ where $zI - \Lambda$ is diagonal, so

$$\left\| (zI - A)^{-1} \right\| = \left\| V(zI - \Lambda)^{-1}V^{-1} \right\| = \|V\| \, \|V^{-1}\| \, \left\| (zI - \Lambda)^{-1} \right\|$$
$$= \kappa(V) \left\| (zI - \Lambda)^{-1} \right\| = \kappa(V)\,\mathrm{dist}(z, \Lambda(A))^{-1} \geq \mathrm{dist}(z, \Lambda(A))^{-1}$$

since $\kappa(A) \geq 1$ for any matrix A. Note that this inequality is tight if and only if $\kappa(V) = 1$ for some V that diagonalizes A, which is equivalent to the normality of A. $\blacksquare$

2.3 ε-Pseudospectra

Perhaps the most useful method for analyzing behavior of matrices and their normality is the concept of its ε-pseudospectrum, which is a generalization of the spectrum.

Definition 2.13 *Given $\varepsilon > 0$, the ε-pseudospectrum of A, denoted $\Lambda_\varepsilon(A)$, is the subset of $\mathbb{C}$ with $\|(zI - A)^{-1}\| > \varepsilon^{-1}$. Equivalently, this is the set $\{z \in \mathbb{C} \mid \|\mathcal{R}(z, A)\| > \varepsilon^{-1}\}$. Note that these sets depend on the choice of norm used.*

In any norm, the spectrum $\Lambda(A)$ is a limit of the ε-pseudospectrum of A. Formally, this is $\lim_{\varepsilon \to 0} \Lambda_\varepsilon(A) = \Lambda_0(A) = \Lambda(A)$. Many useful results attained from eigenvalue and spectral analysis of A are limiting cases as $\varepsilon \to 0$ of more general properties possessed by $\Lambda_\varepsilon(A)$ [40]. For the remainder of this discussion, the focus will be exclusive to 2-norm (Euclidean norm) pseudospectra.

When the norm chosen is the Euclidean norm, an alternate formulation of these sets is given by $\{z \in \mathbb{C} \mid \sigma_m(zI - A) < \varepsilon\}$ where σ_m is the smallest singular value. Also, $\Lambda_\varepsilon(A)$ is the set of all values z for which z is an eigenvalue of a perturbed matrix $A + \delta A$ where $\|\delta A\|_2 \leq \varepsilon$. An analogous definition for the ε-pseudospectrum of Banach space operators and rectangular matrices is also possible [42].

The ε-pseudospectral contours, which are the sets of $z \in \mathbb{C}$ such that $\|(zI - A)^{-1}\|^{-1} = \varepsilon$, may be found through different techniques including resolvents, singular values, images of circles of different radii, spectral radii, etc [37]. Each formulation provides a different insight into the properties being investigated. Use of the resolvent norm, however, is perhaps the most geo-

metric in nature. An example of a *pseudospectral portrait* for a few matrices, consisting of the eigenvalues and a few pseudospectral contours, is shown in Figure 2.2.
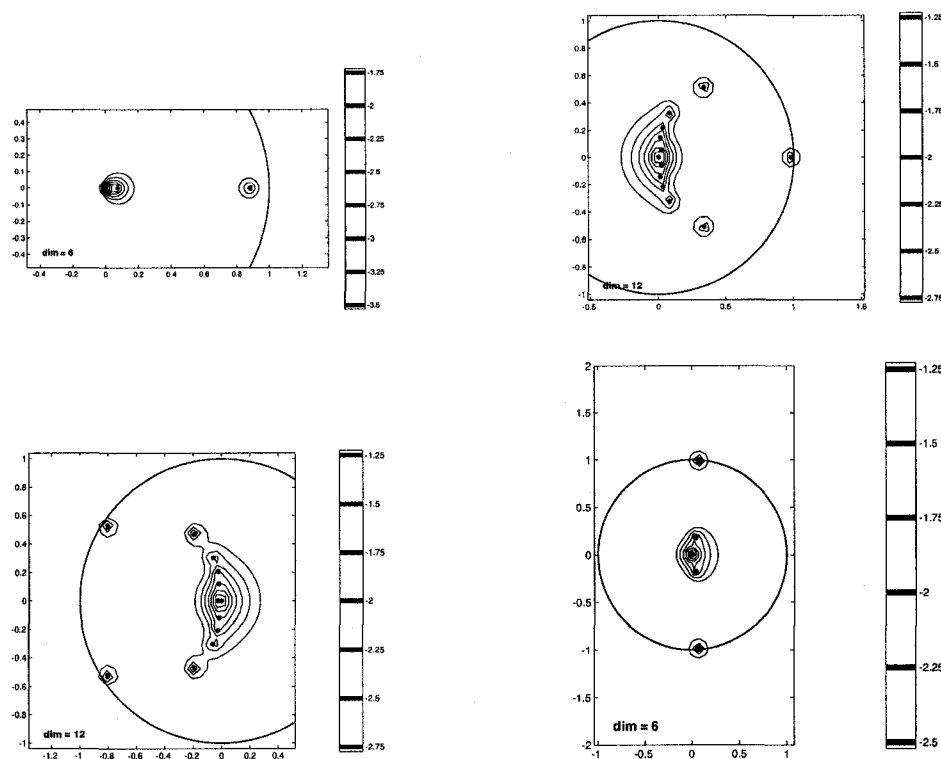

Figure 2.2 Example Pseudospectral Portraits. The unit circle and ε-pseudospectra of approximations to different Schur stable monodromy operators are shown above. Each portrait corresponds to a constant coefficient DDE $(y)(t) = ay(t) + by(t - 1)$ whose coefficients are identified by asterisks in Figure 1.2.

The pseudospectral sets can be ordered by inclusion with $\Lambda_{\varepsilon_1}(A) \subset \Lambda_{\varepsilon_2}(A)$ if $\varepsilon_1 < \varepsilon_2$, which implies that $\Lambda(A) \subset \Lambda_\varepsilon(A)$ for any $\varepsilon > 0$. However, even for small choices of ε, the associated pseudospectrum may be much larger than the union of discs of radius ε about the spectrum when the matrix under investigation is far from normal. Examples of this, as well as the nested structure can be seen in Figure 2.1.

When a value $\lambda \in \mathbb{C}$ has the property that $\lambda \in \Lambda_\varepsilon(A)$, then λ is called an *ε-pseudoeigenvalue*. This means λ is an eigenvalue of a matrix $A + \delta A$ with $\|\delta A\| < \varepsilon$. Correspondingly, there is an eigenvector, ψ, of $A + \delta A$ for $\|\delta A\| < \varepsilon$ associated with λ. Such a vector is called an *ε-pseudoeigenvector*. Note that $(A + \delta A)\psi = A\psi + \delta A\psi = \lambda\psi$, so $A\psi = \lambda\psi - \mathcal{O}(\varepsilon)\psi$. Since ε is typically small, the last term is negligible and ψ almost behaves like an eigenvector of A. This language provides a setting in which linear dynamical system behavior in finite times can be discussed; it makes up for the shortcoming of eigenvalues for evaluating behavior in an exclusively asymptotic sense.

Numerical Computation

Pseudospectra are an analytic measure of non-normality, and they are a tool, both graphical and numerical, for quantifying it and observing its effects. A variety of schemes are available in order to produce pseudospectral data numerically, a property which is of increasing utility in applied mathematics.

Since the graph of the function f_A defined in Equation 2.1 of represents a surface over $\mathbb{C}$ and encodes useful information about a matrix or operator, it has a number of uses. A simple way to create pseudospectral plots is to compute values of f_A at grid points over $\mathbb{C}$ and interpolate the level curves of f_A. This is done by creating a mesh $\{z_{kl} = (x_k, y_l)\}$ around the spectrum of $A \in \mathbb{C}^{n \times n}$ and computing $\|(z_{kl}I_n - A)^{-1}\|$. Figure 2.3 illustrates results for the matrix

$$
S = \begin{bmatrix}
-0.30045526 & 0.66407874 & 0.24987095 & 0.47542405 \\
0.04381585 & -0.09397878 & -0.10034632 & 0.59011142 \\
0.54553751 & 0.00158422 & -0.34477036 & -0.26069051 \\
0.05317001 & -0.20323736 & 0.77459556 & -0.33993500
\end{bmatrix}
\tag{2.2}
$$

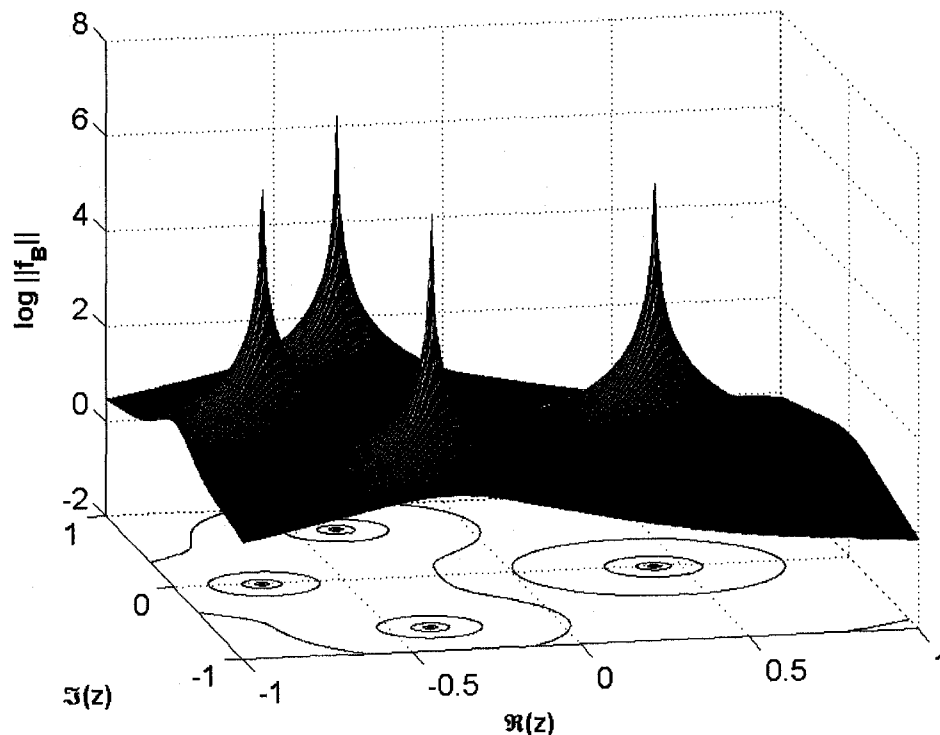for which $\Lambda(S) \approx \{0.42, -0.74, -0.38 \pm 0.69i\}$.

Figure 2.3 A surface corresponding to the logarithm of function f_S for the Schur stable matrix (2.2) over the square $[-1,1]^2 \subset \mathbb{C}$. Projection of level curves for $1, 2, \ldots$ onto the plane are shown. These correspond to $\Lambda_\varepsilon(A)$ for

$$\varepsilon = 10^{-1}, 10^{-2}, \ldots.$$

Efficient algorithms exist to find the ε-pseudospectral contours by way of the singular value decomposition of A [37]. The schemes compute the SVD factorization of $(z_{kl}I_n - A) = U\Sigma V^*$ at each grid-point and storing σ_m, the smallest singular value. More refined, computationally accurate and efficient algorithms for generating these sets are given in [37], and are incorporated into the Matlab package Eigtool [41].

2.4 Non-Normal Matrices

Matrices which are not normal can display an array of behavior which is not possible in normal systems, where eigenvectors can be taken as or-

thogonal. Highly non-normal matrices are characterized by the existence of non-modal transient behavior, which is not predicted by the eigenvalues. This results from the 'inefficiency' of choosing coefficients to represent the matrix in a basis of is eigenvectors. Superposition may lead to accretion or cancelation of value which is reflected in, for example, large short-term growth.

For example, let

$$
A = \begin{bmatrix} .8 & 0 & 0 \\ 0 & .6 - .5i & 0 \\ 0 & 0 & .6 + .5i \end{bmatrix} \qquad V = \begin{bmatrix} -0.6241 & -0.7911 & -0.6312 \\ 0.6662 & 0.5634 & -0.7360 \\ -0.4082 & -0.2383 & -0.2449 \end{bmatrix} \qquad (2.3)
$$

and define $B = VAV^{-1}$. Recall that similar matrices have the same eigenvalues.

The standard basis is a set of eigenvectors for A, while V is a matrix of eigenvectors of B. The standard basis, that is, the identity matrix, has a condition number of 1 while $\kappa(V) \approx 9.14$. Since both of their eigenvalues, the diagonal entries of A, are within $\mathbb{D}$, they are Schur stable, and both decay in the limit. Figure 2.4 demonstrates the difference in norm behavior over the first ten powers, however. Matrix B shows transient growth though it is asymptotically stable.

Stability concerns associated with non-normality

Resonance and amplification for finite intervals of time may arise from non-orthogonal eigenvectors. Although the eigenvalues alone determine theoretical stability in the asymptotic limit, practical problems involve linearizations of more complex systems, and behavior in finite time may be of concern for bifurcation analysis. Nonlinear terms coupled with large transient growth may change the dynamical trajectory of the system [23]. In this case, a lin-
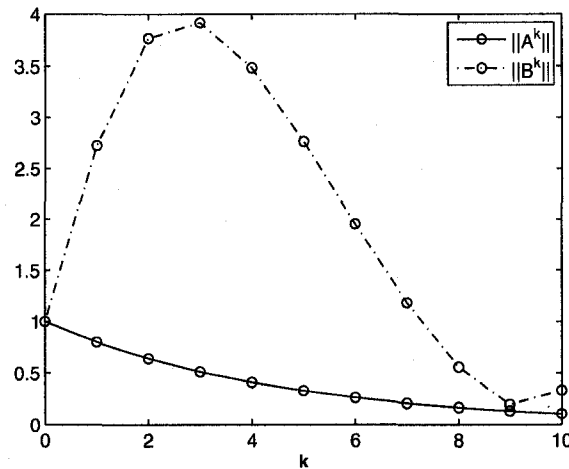
Figure 2.4 Norms of Powers: Normal vs. Non-normal Matrices. Shown above are the norms of the first ten powers of Schur stable matrices A and $B = VAV^{-1}$ given in Equation (2.3). The normal matrix, A, decays geometrically according to powers of $\|A\|$. Matrix B is non-normal and experiences growth for four iterations as well as oscillation.

ear model may not predict the more complex behavior of the system it was intended for. Measuring the non-normality of the linear model can reveal transient growth that may indicate this failure of linearization.

A primary concern for DDEs is stability. One way of solving DDEs by successively applying the monodromy operator $\mathcal{U}$ as discussed previously. In an approximation scheme, a square matrix U may approximate $\mathcal{U}$, and the process becomes one of matrix iteration. Stability is expected when $\Lambda(U) \subset \mathbb{D}$. However, no growth bound on powers of U can be established from $\Lambda(U)$ alone; the eigenvalues only provide information about an equivalence class of similar matrices.

To build toward establishing lower bounds which hold for iteration of both normal and non-normal matrices, it is necessary to associate another useful number with a matrix.

Definition 2.14 *The* Kreiss constant *for a matrix* $A \in \mathbb{C}^{n \times n}$ *is defined as the*

quantity

$$\mathcal{K}(A) = \sup_{z>1}(|z| - 1) \left\| (zI - A)^{-1} \right\|_2.$$

The Kreiss constant is the product of two positive numbers, the distance of a point $z \in \mathbb{C}$ from the unit circle and the value of the resolvent norm at that point, maximized over all choices of z outside the closed disc. For a normal matrix, $\mathcal{K}(A) = 1$ as these two quantities are reciprocal. When A is non-normal, the resolvent norm at a point z outside the unit disc can be much larger than the distance from z to the disc, and consequently $\mathcal{K}(A) > 1$. This fact can be used as an indicator of non-normality. It also useful in cleanly phrasing bounds on the behavior of matrix powers in the following theorems, the first of which is known as the *Kriess Matrix Theorem*. Proofs of the next three statements can be found in [40].

Theorem 2.15 *For* $A \in \mathbb{C}^{n \times n}$, *if* $\left\| (zI - A)^{-1} \right\| = \frac{K}{|z|-1}$ *for some* $K > 1$ *and* z *outside the unit circle, then*

$$K < 1 + |z|(K - 1) \leq \sup_{k \geq 0} \left\| A^k \right\|. \tag{2.4}$$

Maximizing the left hand side of this inequality, a lower bound is attained yielding

$$\mathcal{K}(A) \leq \sup_{k \geq 0} \left\| A^k \right\|. \tag{2.5}$$

This theorem provides important insight into the iterated power norm. Basically, it states that if for some $\varepsilon > 0$, the ε-pseudospectrum of a matrix leaves the unit circle to a distance larger than ε, growth in norm of the iterated matrix should be expected. Said another way, suppose that for some matrix A and choice of $\varepsilon > 0$, there is a point $z \in \mathbb{C} \backslash \mathbb{D}_{1+\varepsilon}$ for which z is an ε-pseudoeigenvalue of A. Then $\mathcal{K}(A) > 1$ and some growth in norm of A will occur as powers are successively taken.

It is natural to wonder just how large this growth may be. A simple upper bound on any square iterated matrix is the bound $\|A^k\| \leq \|A\|^k$ with equality if and only if A is normal [22]. A tighter upper bound on behavior is also given in terms of the Kreiss constant.

Theorem 2.16 *For any square matrix,*

$$\|A^k\| \leq e(k+1)\mathcal{K}(A). \tag{2.6}$$

With the two inequalities given in Equations (2.5) and (2.6), the maximum transient growth of a matrix is bounded. Illustrated in Figure 2.5 are the relationships between the quantities $\mathcal{K}(A)$, $\|A^k\|$, and $\|A\|^k$ for a stable matrix A with $\mathcal{K}(A) > 1$.
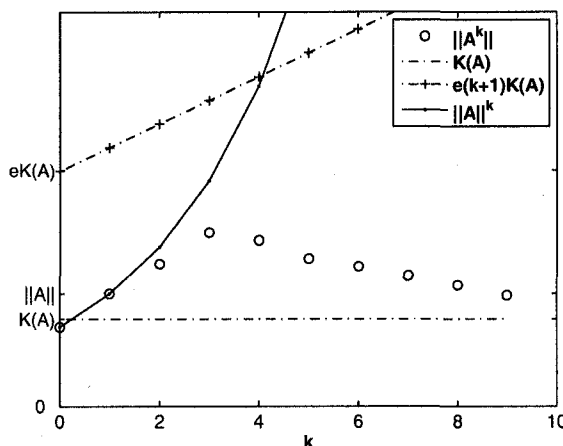

Figure 2.5 Bounds on Matrix Norm Behavior in Terms of Kreiss Constant. Depicted above is the relationship between iterated powers of a matrix A and the Kreiss constant. The norm of A^k is always below the line $e(k+1)\mathcal{K}(A)$, and the line $\mathcal{K}(A)$ is always below the power of A with largest norm.

Chapter 14 of [40] provides a discussion of bounds on the number of iterations over which growth behavior may occurs, a subject which will not be discussed here.

3 Approximation and Computer Representation

Differential equations take a variety of forms such as ordinary, partial, functional, or delay types. All, however, reflect problems of continuous mathematics. Computers cannot store continuous functions except by restricting the class of functions, and methods of representing continuous systems as discrete ones have been established. That is, in order to find practical solutions, numerical analysis must be done. It is essential that the equations be discretized and be represented appropriately in order that the results obtained from them be consistent with the continuous equation from which they were derived.

The purpose of this section is to present techniques used to put the DDEs discussed in the first section into a context in which the matrix content of the second section is relevant. Specifically, the goal is to have a way of approximating DDEs by finite systems of linear equations which may be solved numerically.

3.1 Discretization, Collocation, and Interpolation

The independent variable, t, in DDE (1.3) is continuous. Again, periodicity $A(t + \tau) = A(t)$ and $B(t + \tau) = B(t)$ in Equation (1.3) is assumed. The monodromy operator may then be defined by Equation (1.7), which cuts the range of time variables into pieces of length τ, the delay period of the DDE. Each interval $[0, \tau]$ is the domain of a function on which the monodromy operator acts.

To numerically compute y by solving $y = \mathcal{U}\phi$ for initial data ϕ, a finite set of nodes $\{t_k\}$ in the domain $[0, \tau]$ may be specified at $y|_{t_k} = \mathcal{U}\phi|_{t_k}$. This is a *collocation* method. The numerical scheme used selects points which are

asymptotically clustered at the endpoints of the interval $[0, \tau]$. In particular, the Chebyshev extreme points [38] are selected. For a selection of $n+1$ points, these points in the interval $[-1, 1]$ are given by the formula $x_j = \cos \frac{j\pi}{n}$ ($j = 0, \cdots, n$) with $x_0 = 1$ and $x_n = -1$ so that the points are ordered descendingly. To shift these points to the appropriate interval, the $n + 1$ Chebyshev nodes for the interval $[0, \tau]$ are defined by

$$t_j = \frac{\tau}{2} \left[1 + \cos \frac{j\pi}{n} \right] \quad j = 0, \cdots, n. \tag{3.1}$$

Collocation, in particular, is a method of finding coefficients a_k in an expansion

$$f(t) = \sum_{k=0}^{n} a_k f_k(t)$$

so that an equation $L[f(t_j)] = 0$ is satisfied at nodes $\{t_j\}_0^n$. In seeking coefficients, the task is to find a solution to the equation, f, in a basis of functions $\{f_j\}_0^n$ where the functions f_j are chosen.

For example, these $n+1$ functions could be Lagrange Polynomials based at the Chebyshev extreme points, so that there is an nth degree polynomial associated with values at each node. These functions, called *Chebyshev-Lagrange polynomials* are given by the formula

$$f_j(t) = \prod_{\substack{k=0 \\ k \neq j}}^{n} \frac{t - t_k}{t_j - t_k} \qquad (j = 0, \ldots, n) \tag{3.2}$$

where $\{t_k\}$ are Chebyshev extreme points. Formula (3.2) is a concise way of writing these polynomials, but is not good for practical evaluation [27]. Efficiency and accuracy of evaluation of these and other functions is discussed in [17, 6]. It is clear from the form of Equation (3.2) that $f_j(t_k) = \delta_{jk}$. This last fact provides a clean way of interpolating a given function $\phi : [0, \tau] \to \mathbb{C}$;

if $\hat{\phi} = \{\phi(t_k)\}_0^n$ are its values at the $n+1$ nodes, then $p(t) = \sum_0^n \phi(t_k) f_k(t)$ is a polynomial interpolant which matches ϕ at each node. It will be convenient to denote by I_n the $n+1$ dimensional polynomial interpolant operator which sends a function to its degree n polynomial interpolating function.

Polynomial interpolation of smooth functions at Chebyshev points has the important property that it is exponentially accurate. In particular, the residual value $\|\phi - p\| = \|\phi - I_n\phi\|$ decreases exponentially with increasing n when ϕ is an analytic function [36]. Such a property has come to be known as *spectral accuracy* [38].

For discretized data which is known at Chebyshev points, differentiating interpolants and getting the derivative values at the Chebyshev points is computable by applying a *Chebyshev differentiation matrix* provided in [38]. Applying such a matrix corresponds to interpolating by a degree n polynomial, differentiating that polynomial, and then evaluating the result at the $n+1$ Chebyshev points. It will be denoted by D, with $D \in \mathbb{C}^{n+1 \times n+1}$ for $n+1$ Chebyshev nodes.

3.2   Discretizing the monodromy operator

Suppose that $\hat{\phi}$ is an interpolant of the history function ϕ. For numerical convenience, it is stored as a list of $n+1$ values at the collocation points on interval $[-\tau, 0]$. These coefficients form a vector, $\hat{\phi} \in \mathbb{C}^{n+1}$, which is a slight abuse of notation. What is sought is the vector $\{y_j\}_0^n \in \mathbb{C}^{n+1}$ of collocation values so that the interpolant $\hat{y}$ is an approximate solution to the DDE on the next interval of length τ. The list of values of the interpolant $\hat{y}$ is also denoted $\hat{y} \in \mathbb{C}^{n+1}$. The time derivative $\dot{y}$ in the continuous equation is approximated by $D\hat{y}$, the derivative of its polynomial interpolant.

Multiplication by $A(t)$ and $B(t)$ in the scalar DDE (1.3) are written as matrices $M_A, M_B \in \mathbb{C}^{n+1 \times n+1}$ with $(M_A)_{jj} = A(t_j)$ and $(M_B)_{jj} = B(t_j)$ where

$j = 0, \ldots, n-1$ [10]. The final rows of these matrices, as well as D, are modified to encode the implicit boundary condition, ensuring that the solution begins at the appropriate place. In particular, $D_{n,:}$, $(M_A)_{n,:}$, $(M_B)_{n,:}$ are set to zero since the value of y_n is determined by ϕ_0. Also, D_{1n} and $(M_B)_{1n}$ are taken as the identity, which in the scalar case is 1, to represent ϕ_0 as the starting point. All other entries of M_A and M_B are zero.

With these matrices, the linear system approximating the continuous DDE has the form

$$D\hat{y} = M_A\hat{y} + M_B\hat{\phi}.$$

Solving this for $\hat{y}$ gives $\hat{y} = (D - M_A)^{-1} M_B\hat{\phi} = U\hat{\phi}$ so that $U \in \mathbb{C}^{n+1 \times n+1}$ is a constructed rank $n + 1$ approximation to the monodromy operator $\mathcal{U}$ [8, 11], and it is in the basis of Chebyshev-Lagrange polynomials. This approach generalizes to higher order DDEs and systems of DDEs as well as those with multiple delays [10]. The Matlab suite ddec implements the type of numerical scheme discussed above [9], and is used for all numerical approximations to $\mathcal{U}$ in this thesis, including those used in previous figures such as Figure 2.2.

An important question to ask now is whether the behavior in the finite dimensional approximation U converges to that of $\mathcal{U}$ as $n \to \infty$. A treatment of this question shows that the finite dimensional approximation converges in the sense that initial value solutions converge [21]. For the monodromy operator itself approximated by the scheme discussed above, the monodromy matrices converge to the monodromy operator in the sense that eigenvalues are close [8], a topic surveyed next.

Accuracy of Eigenvalues

An essential topic for the stability of DDEs is whether the largest eigenvalues of a numerical approximation to $\mathcal{U}$ are accurate. This subsection demon-

strates good convergence of the scheme discussed above. Note that in simple cases, it may be possible to analytically find the Floquet multipliers of the DDE, which are exactly the eigenvalues of $\mathcal{U}$. An example is given below, in Hurwitz form. This form is chosen to spread out the eigenvalues of computed U, and produce a more interesting picture. The accuracy of the numerical scheme used to generate approximations is then more clearly visible.

Consider a simple scalar constant coefficient DDE with no undelayed term

$$\dot{y}(t) = -y(t-1). \tag{3.3}$$

To compute the characteristic multipliers, the Laplace transform is used, that is, $y(t) = e^{st}$. Note that $y(t+1) = e^s e^{st}$ so that e^s is like a Floquet multiplier by Theorem 1.6. Substitution of this assumed solution into Equation (3.3) gives $se^{st} = -e^{s(t-1)}$, so s satisfies $se^s = -1$. The solutions to this equation can be found by evaluation of the multi-valued inverse of $w = f(z) = ze^z$, known as the Lambert W function, at the point $w = -1$ [14]. In Figure 3.1, these solutions are compared to the eigenvalues of a rank 60 approximation of $\mathcal{U}$ generated by the numerical scheme (see Figure 1.1). The eigenvalues of U are taken to the appropriate region of $\mathbb{C}$ by a conformal map F:

$$z \mapsto \left(\log \alpha \frac{1-z}{1+z} \right)^{-1}, \quad \alpha \in \mathbb{C} \tag{3.4}$$

which takes the interior of the unit disk to the left half-plane. The largest eigenvalues of U line up well with the analytically found Floquet multipliers.

These results are experimental in nature. However, it demonstrates that a well implemented approximation to $\mathcal{U}$ correctly obtains the part the spectrum with largest modulus. These eigenvalues correspond to the points with
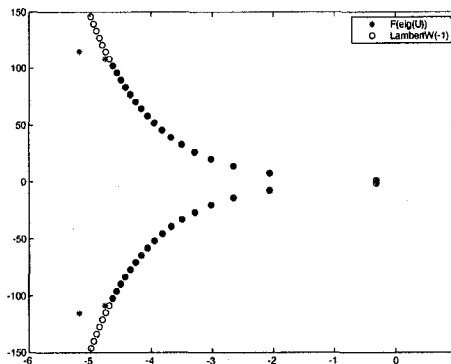
Figure 3.1 Eigenvalues of a Monodromy Matrix: Computed vs. Analytic. The accuracy of the approximated eigenvalues for $\mathcal{U}$ compared with those analytically known. The circles are exact multipliers computed by the Lambert W function. Asterisks indicate the eigenvalues of a monodromy matrix, conformally mapped to the left half plane by (3.4) with $\alpha = 2$. The largest eigenvalues of U coincide with the analytic Floquet multipliers, but eventually become inaccurate.

largest real part in Figure 3.1. This suggests that spectral analysis on finite dimensional matrix approximations will be useful for assessing spectral properties of the infinite dimensional monodromy operator.

3.3 Normality of $\mathcal{U}$ and the Need for an Inner Product

The definition of pseudospectra in Definition 2.13 requires only a norm, and hence is applicable to all Banach spaces. In a generic Banach space, the associated dual space is not identifiable in any geometrically meaningful way with the original space. As a result, the definition of normality, namely $A^*A = AA^*$, is meaningless since $\mathrm{dom}(A^*) \neq \mathrm{range}(A)$. In fact, the question of non-normality is different than the ability to generate a skewed set of pseudospectra. In order to define "normality" itself, it is necessary that the space on which the objects act has either an inner product or some idea of angles between functions. In summary, normality should only be considered in a Hilbert space, a complete inner product space.

The operator $\mathcal{U}_0$ solving the standard form of the DDE with constant delay acts naturally on the set of continuous functions $C[0,\tau]$. This makes $\mathcal{U}$ an operator on a Banach space, complete under the natural norm $\|\cdot\| = \|\cdot\|_\infty$. This norm can be used to generate a set of pseudospectral curves around the spectrum of $\mathcal{U}$, but it cannot be used to define an inner product. The existence of an extension of $\mathcal{U}_0$ to an inner product space has been established in subsection 1.3. However, there is more flexibility available in selecting the Hilbert space than is suggested in subsection 1.3. A positive weight function, $w(x) > 0\, ae$, may be chosen in determining the inner product and norm. The inner product for functions of the space $L_w^2[0,\tau]$ will be denoted $\langle\cdot|\cdot\rangle_w$ and is defined by

$$\langle f|g\rangle_w = \int_0^\tau f^*(t)g(t)w(t)dt. \tag{3.5}$$

Note also that $\mathcal{U}$ is not a purely integral operator, acting not simply on $L_w^2[0,\tau]$, but on $\mathbb{C}\oplus L_w^2[0,\tau]$. This is because $\mathcal{U}$ requires point-wise evaluation of the function to which it is applied, implying that $\mathcal{U}$ is not a bounded operator with the weighted inner product defined above. Instead, the domain of $\mathcal{U}$ in Theorem 1.9 generalized to the space $\mathbb{C}\oplus L_w^2[0,\tau]$ with inner product

$$\langle(\alpha,f)|(\beta,g)\rangle_{w,\omega} = \omega\alpha^*\beta + \langle f|g\rangle_w \tag{3.6}$$

where $\omega \geq 0$ is a weight assigned to the product of elements of $\mathbb{C}$.

Theorem 3.1 *The monodromy operator $\mathcal{U}$ acts boundedly on the inner product space $\mathcal{H} := \mathbb{C}\oplus L_w^2[0,\tau]$ with the norm induced by the inner product given in Equation (3.6).*

Numerical Inner Product

In practical implementation, the functions of the space $\mathcal{H}$ are not known exactly. They are instead approximated by their Chebyshev-Lagrange interpolants. This generates the need to approximate the inner product of $\mathcal{H}$ for the vectors representing functions in this particular polynomial basis. The approximate inner product of Equation (3.6) is formulated below where $\phi, \psi \in \mathcal{H}$ and $I_n\phi, I_n\psi$ are their corresponding interpolants:

$$\langle \phi | \psi \rangle_w = \int_0^\tau \phi(t)\psi(t)w(t)dt \approx \int_0^\tau (I_n\phi)(t)(I_n\psi)(t)w(t)dx$$

$$= \sum_{\substack{j=0 \\ k=0}}^{n} \phi(t_j)\psi(t_k) \int_0^\tau f_j(t)f_k(t)w(t)dt = \hat{\phi}(W^H W)\hat{\psi}$$

where W^H denotes the hermitian conjugate of the matrix W and $\{f_j\}$ are the Chebyshev-Lagrange polynomials of Equation (3.2) based at the $n + 1$ Chebyshev nodes. To include the effect of the initial points $\phi(0)$ and $\psi(0)$, the constant ω is added to the entry $W^H W_{1,1}$. The weight matrix, W, can then be found via Cholesky factorization of $W^H W$, which is hermitian positive definite [39].

The entries of $W^H W$ can be computed for a particular choice of w by taking the w-weighted inner product of Chebyshev-Lagrange polynomials, the basis elements in which U is written and functions ϕ are represented:

$$(W^H W)_{jk} = \delta_{jk}\omega + \int_0^\tau f_j(x)f_k(x)w(x)\,dx. \tag{3.7}$$

One wants to compute entries 3.7 as accurately and efficiently as possible. One may take advantage of the special properties of Chebyshev-Lagrange polynomials. A barycentric formula for these polynomials is used to represent these functions efficiently [6]. Then, a gaussian quadrature rule scheme

applied to find the integrals of a weighted product of these functions over the interval $[0, \tau]$ [12]. Cholesky factorization of this matrix is then computed, resulting in the weight matrix W.

The constant ω and function w in Equation 3.6 will be taken as zero and 1, respectively, for the remainder of this thesis. The former choice affords the initial point no weight in addition to that which it is given in the integral. The latter choice corresponds to not weighting the L^2 space from which the functions come.

3.4 Eigenvectors of the monodromy matrix

The monodromy operator associated with a single delay DDE depends on the length of the delay τ and on the coefficients $A(t)$ and $B(t)$. However, in the case of a scalar DDE with τ-periodic coefficients, the eigenvalues of the operator depend only on the means of these coefficients over one period. This is demonstrated through solutions to the DDE in the following theorem.

Proposition 3.2 *Consider a scalar DDE problem with time-dependent periodic coefficients and simple fixed delay τ. This equation takes the form*

$$\dot{y}(t) = A(t)y(t) + B(t)y(t - \tau) \tag{3.8}$$

where $A(t + \tau) = A(t)$ and $B(t + \tau) = B(t)$. Define the average coefficients

$$\overline{A} = \frac{1}{\tau} \int_0^\tau A(t)\, dt \quad and \quad \overline{B} = \frac{1}{\tau} \int_0^\tau B(t)\, dt. \tag{3.9}$$

Then the Floquet multipliers (and hence eigenvalues of $\mathcal{U}$) associated with the **DDE**

$$\dot{y}(t) = \overline{A}y(t) + \overline{B}y(t - \tau) \tag{3.10}$$

are the same as those associated with Equation (3.8).

Proof. It will be shown that a formula for the eigenvalues of $\mathcal{U}$ associated to Equation 3.8 is dependent only on the coefficient means 3.9. Suppose eigenvalue $\lambda \in \Lambda(\mathcal{U})$ has eigenfunction $y_\lambda(t)$. If $y_\lambda(t)$ is the initial data function on the interval $[0, \tau]$, then $\lambda^k y_\lambda(t - k\tau)$ is a solution to 3.8 on the interval $[(k-1)\tau, k\tau]$. The monodromy operator acts on y_λ by rescaling it by the value of the associated eigenvalue, and then translating it by τ to the right because $(\mathcal{U}y_\lambda)(t) = \lambda y_\lambda(t - \tau)$.

On the interval $[0, \tau]$, one has

$$\frac{d}{dt}(\lambda y_\lambda(t)) = A(t)(\lambda y_\lambda(t)) + B(t)y_\lambda(t).$$

so $z = y_\lambda$ solves the ODE problem

$$\dot{z}(t) = \left[A(t) + \lambda^{-1}B(t)\right]z(t), \qquad (\lambda \neq 0). \tag{3.11}$$

Because this ODE is scalar, it can be solved the standard way, by integration, yielding

$$z(t) = e^{\int_0^t A(s) + \lambda^{-1}B(s)\,ds}z(0)$$

However, the solution to the eigenvalue problem has the property that $z(\tau) = \lambda z(0)$ for the sake of continuity at endpoints. This gives

$$z(\tau) = e^{\int_0^\tau A(s) + \lambda^{-1}B(s)\,ds}z(0) = \lambda z(0)$$

or

$$\lambda = e^{\int_0^\tau A(s) + \lambda^{-1}B(s)\,ds}$$

when $z(0) \neq 0$. This is precisely $\lambda = \exp[\tau\overline{A} + \tau\lambda^{-1}\overline{B}]$, so λ only depends on the means of $A(t)$ and $B(t)$. $\blacksquare$

A key idea of this proof is that the DDE eigenvalue problem (for a nonzero eigenvalue) is equivalent to a parameter-dependent ODE problem in which the parameter is the eigenvalue. The theorem, however, does not extend to higher dimensional systems precisely because the solution to Equation (3.11) cannot be found for general matrices A and B by exponentiating $\int_0^\tau A(s) + \lambda^{-1} B(s) \, ds$; a more general expansion would be required [33].

This proposition predicts zero-mean perturbations of the DDE coefficients do not affect the spectrum of $\mathcal{U}$, and consequently the eigenvalues of the monodromy matrix U. However, the solutions to the DDEs of Equations (3.8) and (3.10) do differ. The eigenfunctions of the associated $\mathcal{U}$ are indeed affected by zero-mean perturbations. That is, the normality of the monodromy operator are affected by zero-mean perturbations while its spectrum is unaltered. These effects can be explored via pseudospectra.

To investigate non-normality of the monodromy matrices of DDEs, different types of zero-mean perturbations will be applied to constant coefficient scalar DDEs, effectively altering the eigenvectors of U. These types of DDEs will be explored in Section 4.

4 Finding non-normal monodromy operators

A linear, periodic DDE will be called normal or non-normal depending on whether its associated monodromy operator $\mathcal{U}$ is normal or non-normal. This definition depends on an implied choice of Hilbert space on which $\mathcal{U}$ acts. See Section 3.3. In this section, monodromy operators corresponding to the class of scalar, linear, periodic DDEs with non-constant delay coefficients

$$\dot{y}(t) = Ay(t) + B(t)y(t-1) \tag{4.1}$$

will be explored. The coefficient A is constant and $B(t)$ has the form $B_0 + p(t)$ where $p : [0, \tau] \to \mathbb{R}$ is an integrable function *which has zero mean*. The spectrum of the monodromy operator $\mathcal{U}$ is unaltered by $p(t)$ by Proposition 3.2. However, the eigenfunctions associated with $\mathcal{U}$ change, affecting its normality. The effects are illustrated graphically in pseudospectral portraits of approximations to $\mathcal{U}$. The goal is to produce an example of a highly non-normal DDE in the sense that $\Lambda_\varepsilon(U)$ contains parts of $\mathbb{C}$ far from $\Lambda(U)$.

4.1 Application of Weight

The graphical affects of applying the weight matrix W to a monodromy matrix are demonstrated in Figure 4.1 for the DDE (4.1) with $(A, B_0) = (-3.5, -3)$ and $p = 0$. The corresponding rank 60 monodromy matrix is Schur stable $\rho(U) \approx .74$ where $\rho(U) := \max_{\lambda_i \in \Lambda(U)} |\lambda_i|$.

Pseudospectral plots hereafter will not be of U, even if U is referred to in the discussion and caption. Instead, they will be of WUW^{-1}. This change of basis gives the monodromy matrix in the 2-norm basis so that the adjoint and transpose coincide [37]. The reader should assume that references to U
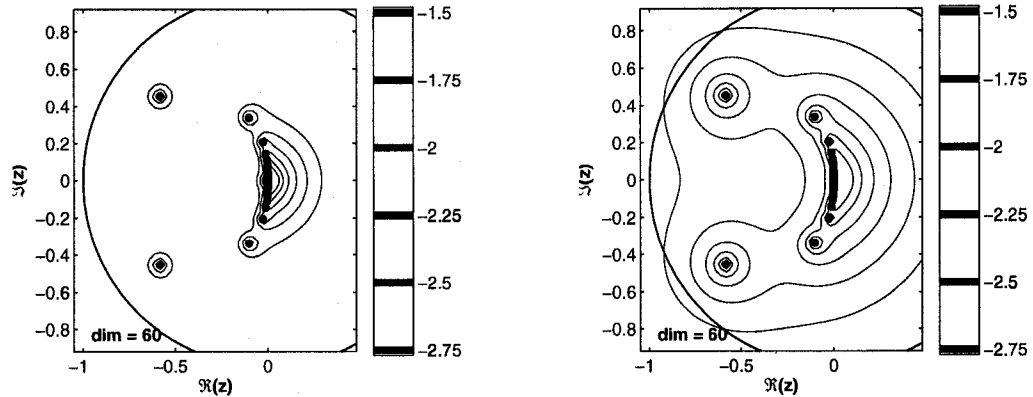
Figure 4.1 Effect of Weighting the Monodromy Matrix on Pseudospectra. The left figure is the pseudospectral portrait of U, unweighted. On the right is the corresponding portrait for the weighted matrix WUW^{-1}. The effect of similarity transform distorts the eigenvectors of U, revealed graphically in the changes of the pseudospectral contours.

actually refer to the basis transformed monodromy matrix WUW^{-1} for the remainder of this discussion unless otherwise specified as 'unweighted'. The weight W is computed for $w = 1$ and $\omega = 0$, as mentioned previously.

There are several ways of measuring the extent of non-normality as discussed in 2.1. Note that applying W to U in Figure 4.1 aids in orthogonalizing the eigenvectors of U as it decreases the eigenvector matrix condition number from about 10^4 to about $4 \cdot 10^3$. However, the Henrici departure, D_H, increases from 3.68 to 20.3 in doing so. Large eigenvector matrix condition numbers for U may not be useful in assessing whether U behaves poorly for certain initial data. Since D_H increases while $\kappa(V)$ decreases in the example of Figure 4.1, neither may be practical in assessing normality in this discussion. Instead, investigation of non-normality will be approached through ε-pseudospectra.

This perspective allows for finding aspects of non-normality which may be of concern to stability analysis of Equation 4.1. It may have solutions which are amplified greatly even though the system is asymptotically stable.

Solutions of this sort would be characterized graphically by $\Lambda_\varepsilon(U)$ extending beyond the boundary of the unit circle for some small $\varepsilon > 0$, and the region of $\mathbb{C}$ into which the $\Lambda_\varepsilon(U)$ extends allows for finding the corresponding ε-pseudoeigenvalue. The associated pseudoeigenvector ϕ_λ then represents the polynomial interpolant of a pseudoeigenfunction of $\mathcal{U}$ associated with Equation 4.1. If $\lambda \in \Lambda_\varepsilon(U)$ is found outside the unit circle, Theorem 2.5 implies that the ϕ_λ will be an initial function which shows growth.

4.2 Known types of errors to avoid

Proposition 3.2 implies that the spectrum of $\mathcal{U}$ should not change under a zero mean perturbation, and neither should the eigenvalues of an approximation to $\mathcal{U}$. However, there are limitations of the numerical scheme used in discretizing $\mathcal{U}$ discussed in Section 3 which must be considered. Accuracy of the interpolation to the coefficients is prerequisite to a good approximation of $\mathcal{U}$

In the numerical scheme, the coefficients A and B are sampled at $n + 1$ points and interpolated by a degree n polynomial. Although the scheme implements spectral methods with good convergence properties for analytic functions, finite approximations may not resolve large changes in the function. This case, in which too few nodes are used, results in the inaccuracy of the largest eigenvalues of U, which is worrisome. Figure 4.3 are $\Lambda_\varepsilon(U)$ and $\Lambda_\varepsilon(U_p)$ where U, U_p are unweighted approximations to the monodromy operators associated with the stable DDEs

$$\dot{y}(t) = -y(t) + (1.3 + p(t))y(t - 1) \tag{4.2}$$

where U is found for $p(t) = 0$ while U_p is found for

$$p(t) = \frac{300}{\sqrt{\pi}}(t - .3)\exp[-100(t - .3)^2] \qquad (4.3)$$

extended with period $\tau = 1$. This perturbation has a shape shown in Figure 4.2. This perturbation to the DDE coefficient results in movement of the
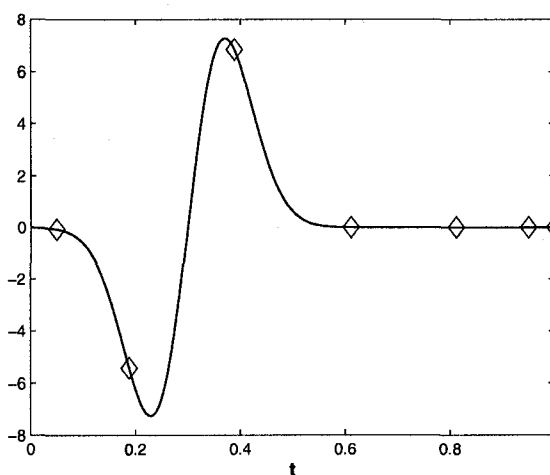

Figure 4.2 A Plot of Function (4.3), a Wave Packet. Above is the zero mean function $p(t)$ given in (4.3) on the interval $[0,1]$. Also shown are the values at the 7 Chebyshev zero points.

largest eigenvalues of U_p (Figure 4.3), which seems inconsistent with Proposition 3.2. However, this is a numerical effect due to poor interpolation of the perturbation. The Chebyshev interpolation points have a minimal density in the middle of the interval $[0,\tau]$ and are symmetric about $\tau/2$, in this case, about $t = 1/2$. For a perturbation like $p(t)$ which is symmetric about some point other than $t \in \{0, \tau/2, \tau\}$, the symmetric interpolation points may fail to represent p adequately. Consequently, the polynomial interpolating this data may not have zero mean, and the computed spectrum of U_p will be inaccurate.

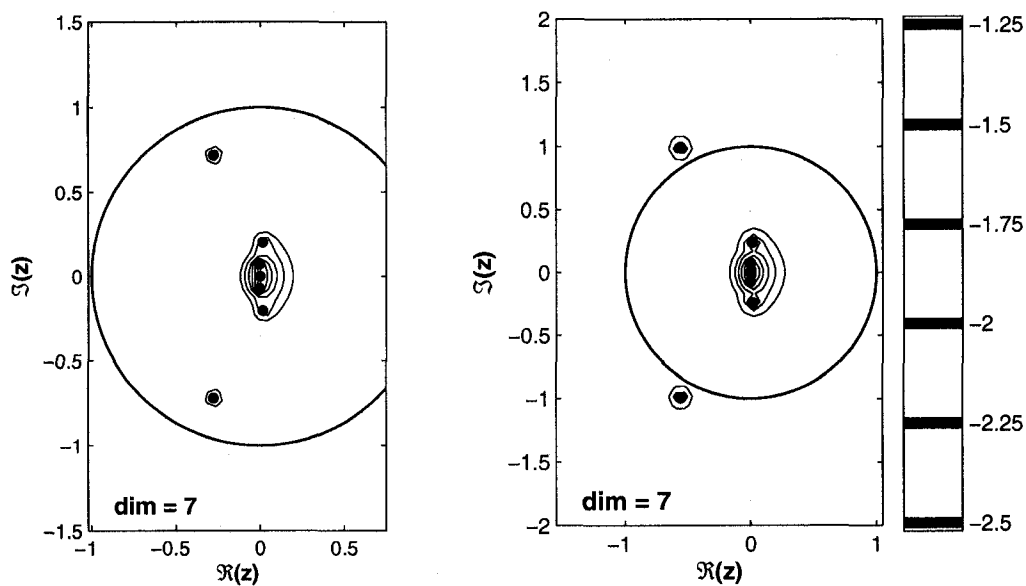Failure to accurately interpolate the perturbation may have effects other

Figure 4.3 A Perturbation Changing Monodromy Matrix Large Eigenvalues.
The left figure shows the spectral portrait of U corresponding to a constant
coefficient stable DDE. On the right, the same 'stable' monodromy matrix
with a perturbed delay coefficient, which is no longer stable. The unit circle
is shown.

than changes in the largest eigenvalues, shown previously. Consider the DDE

$$\dot{y}(t) = (-1 + q(t))y(t - 1) \tag{4.4}$$

where $q(t)$ is a zero-mean function comprised of two gaussian waves, one pos-
itive and one negative. Take, for example, the function

$$q(t) = \frac{5}{\sqrt{\pi}} \left(\exp[-100(t - .7)^2] - \exp[-100(t - .3)^2] \right), \tag{4.5}$$

shown for $t \in [0, 1]$ in **Figure 4.4**. Again, this function has zero mean, and is
extended periodically.

Two rather different sets of eigenvalues are computed for U_q with 6 and 60
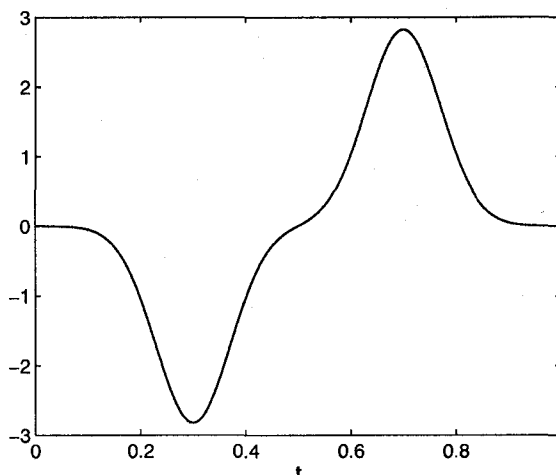
Figure 4.4 A Plot of Function (4.5), a Superposition of Wave Packets. The function given in Equation (4.5) is shown for $t \in [0, 1]$. Note symmetry with respect the midpoint of the interval.

collocation points as shown in Figure 4.5. Note that the latter approximation is nearly the correct spectrum of the unperturbed monodromy matrix associated with $\ddot{y}(t) = -y(t-1)$. Although the largest eigenvalues of U_p are accurate even for low rank approximations, smaller eigenvalues are not.

These situations are rectifiable by increasing the rank of the monodromy matrix. Increasing the dimension of the monodromy matrix U may not be without undesired effects. For example, the problem of underestimation illustrated in Figure 4.5, was avoided by increasing the dimension of U by a factor of 10. In doing so, the eigenvector matrix condition number grows on the order of 10^2. Recall that the monodromy operator is compact, and has only a finite number of eigenvalues outside $\mathbb{D}_\varepsilon$ for any $\varepsilon > 0$ [29]. The numerical scheme used to approximate $\mathcal{U}$ exhibits rapid convergence to the largest eigenvalues, but slow convergence to those within this region [8]. The use of more collocation points means U will have larger numbers of near-zero eigenvalues which may not have the desired accuracy. The eigenvector matrix condition
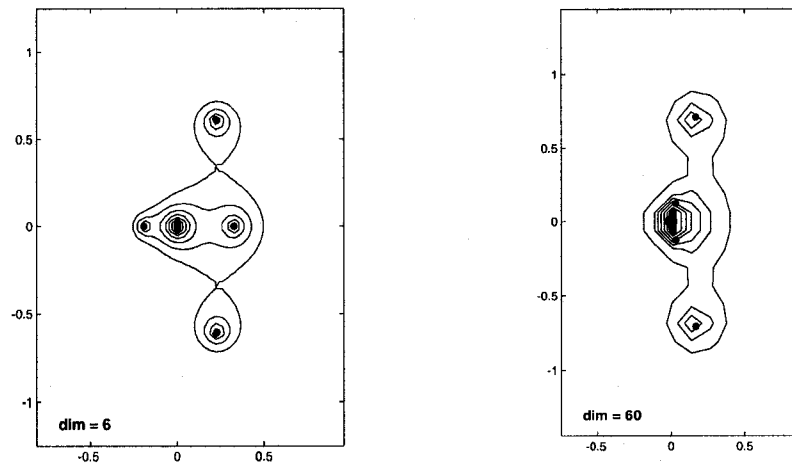
Figure 4.5 A Perturbation Changing Monodromy Matrix Small Eigenvalues. Harmful effects of underestimation as discussed above are shown. A pair of nearly zero eigenvalues split apart and drift away from the origin.

number may not be practical for large dimension approximations to $\mathcal{U}$, as it may simply reflect the inaccuracy of many eigenvectors associated with the eigenvalues near the origin. However, the relationship between compactness, the numerical scheme, and the eigenvector matrix condition number is poorly understood at the current time.

Shown in Figure 4.6 are a sequence of unweighted rank n approximations to U_q of the previous example. It demonstrates that improving the rank of monodromy operator approximations leads to a stable picture of the eigenvalues and pseudospectra. The pseudospectral contours indeed enlarge with increasing dimension, but their overall shape remains the same.

4.3 Perturbations

The perturbation function p can be any zero mean coefficient provided that $p(0) = p(\tau)$ to ensure continuity and periodicity of $B(t) = B_0 + p(t)$. A few choices of p are used here to investigate their effect on U. The emphasis here
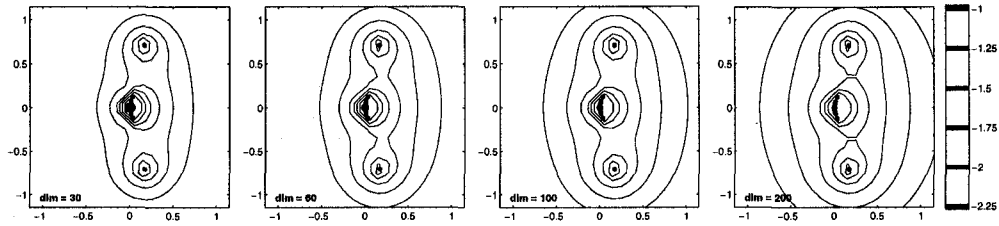
Figure 4.6 Monodromy Operator Approximations with Increasing Rank. For the delay coefficient perturbation $q(t)$ given in Equation (4.5), this plot shows unweighted U_q for DDE (4.4). The rank of these approximations are 30, 60, 100, and 200 (left to right).

is on perturbation only of the delay coefficient. Experimentation with the following perturbations of the non-delay coefficient produced results which were not different enough from the constant coefficient results to be of interest.

Wave Packet Perturbations

A useful type of perturbation has the form $p(t) = C_1(t-C_2)\exp[-C_3(t-C_2)^2]$ restricted to $t \in [0,\tau]$. There are nice properties of this type of perturbation function. It is analytic, and is well represented by the numerical scheme used. Also, the parameters C_i allow for adjusting the amplitude of the perturbation as well as the width and location of its support. Figure 4.7 shows a pseudospectral portrait for the rank 150 weighted monodromy matrix for

$$\dot{y}(t) = -3.5y(t) + (-3 + p(t)))\, y(t-1) \tag{4.6}$$

where

$$p(t) = 500\pi^{-1/2}(t - .3)\exp[-100(t - .3)^2] \tag{4.7}$$

is a wave packet like that of Equation (4.3) in Figure 4.2. Again, this function is extended periodically, but the monodromy operator for a periodic DDE only depends on one period which here is $t \in [0, 1]$.
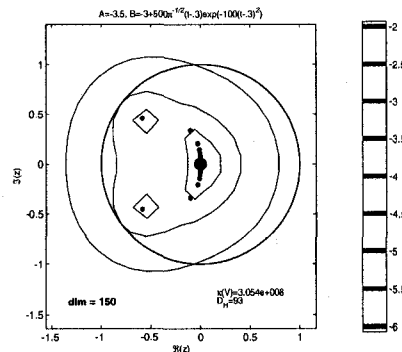
Figure 4.7 Monodromy Pseudospectra for a Wave Packet Perturbation. This is the pseudospectral plot for the monodromy matrix associated to Equation (4.6). This illustrates what is sought: areas outside the unit circle where the resolvent of a stable matrix is large.

It is easily verified that any sum or difference of τ-periodic functions on $[0, \tau]$ with zero-mean also has these properties. Hence, it is possible to apply to B_0 any superposition of appropriate functions. A type of a perturbation which produces interesting examples is the sum of functions like that given in (4.7) having the form

$$q(t) = C_1(t - C_2) \exp[-C_3(t - C_2)^2] + C_4(t - C_5) \exp[-C_6(t - C_5)^2] \qquad (t \in [0, \tau])$$

$$(4.8)$$

and extended τ-periodically. Restrictions should be put on the parameters, such as $C_2, C_5 \in [a, b] \subset [0, \tau]$ and C_3, C_6 large enough to ensure the entire wave is contained in $[0, \tau]$.

The effects on the weighted monodromy matrix of this type are shown in Figure 4.9 where again $(A, B_0) = (-3.5, -3)$ and $\tau = 1$ as in Equation (4.6). The perturbation used, shown in Figure 4.8, is given explicitly by

$$q(t) = \frac{245}{\sqrt{\pi}}(t - .6) \exp[-49(t - .6)^2] + \frac{294}{\sqrt{\pi}}(t - .4) \exp[-49(t - .4)^2]. \qquad (4.9)$$
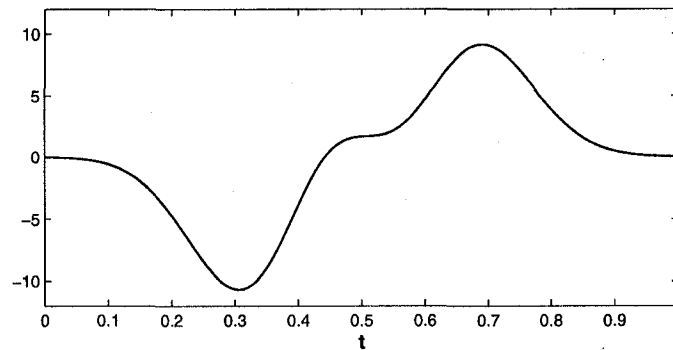
Figure 4.8 Superposition of Wave Packers of Equation (4.9). Shown above is a plot of the function given in (4.9) on the interval $[0, 1]$. It has zero mean, and is extended periodically. Although asymmetric with respect to $t = .5$, 150 Chebyshev nodes are sufficient to accurately represent this function.
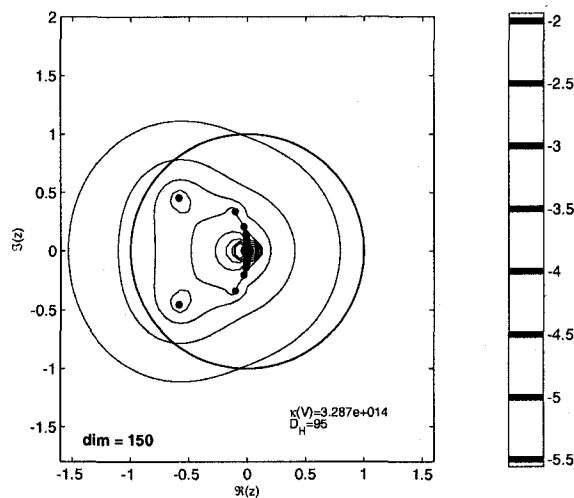

Figure 4.9 Pseudospectra for Perturbation (4.9) on Monodromy Matrix. Shown are pseudospectra for rank 150 monodromy matrix, where U is computed for the DDE with delay coefficient perturbation (4.9). It appears to be very non-normal.

One wonders whether these results, which display non-normality in the monodromy matrix, are dependent on the choices of A and B_0. Figure 2.2 on page 27 shows possibilities for $\Lambda(U)$ based on choices of the pair (A, B_0). For example, $(A, B_0) = (0, -1)$ produces U with two large complex eigenvalues

which have small real part. Also, the choice $(-5, -4)$ gives two large eigenvalue pairs with similar magnitude of imaginary part but different real parts. Finally, an example which gives U with one large purely real eigenvalue is $(-4, 2.5)$ which also has a smaller conjugate pair. A pair $(-1, .4)$ has simply one real large eigenvalue. For a rank 150 approximation of $\mathcal{U}$, each U for these base pairs has over 140 eigenvalues near the origin.

Figures 4.10 and 4.11 show the effects of two different perturbations, both superpositions of mean-zeroed wave packets, applied to B_0 at four different choices of (A, B_0), shown above the plots, within the stability region. All plots in the left column correspond to rank 150 monodromy matrices for DDE (4.1) with coefficients (A, B_0) subject to the perturbation

$$p_1(t) = 49\pi^{-1/2}[5(t - .6)\exp[-49(t - .6)^2] + 6(t - .4)\exp[-49(t - .4)^2]] \quad (4.10)$$

applied to B_0. The right plots correspond to

$$p_2(t) = 49\pi^{-1/2}[7(t - .6)\exp[-49(t - .6)^2] + 10(t - .4)\exp[-49(t - .4)^2]] \quad (4.11)$$

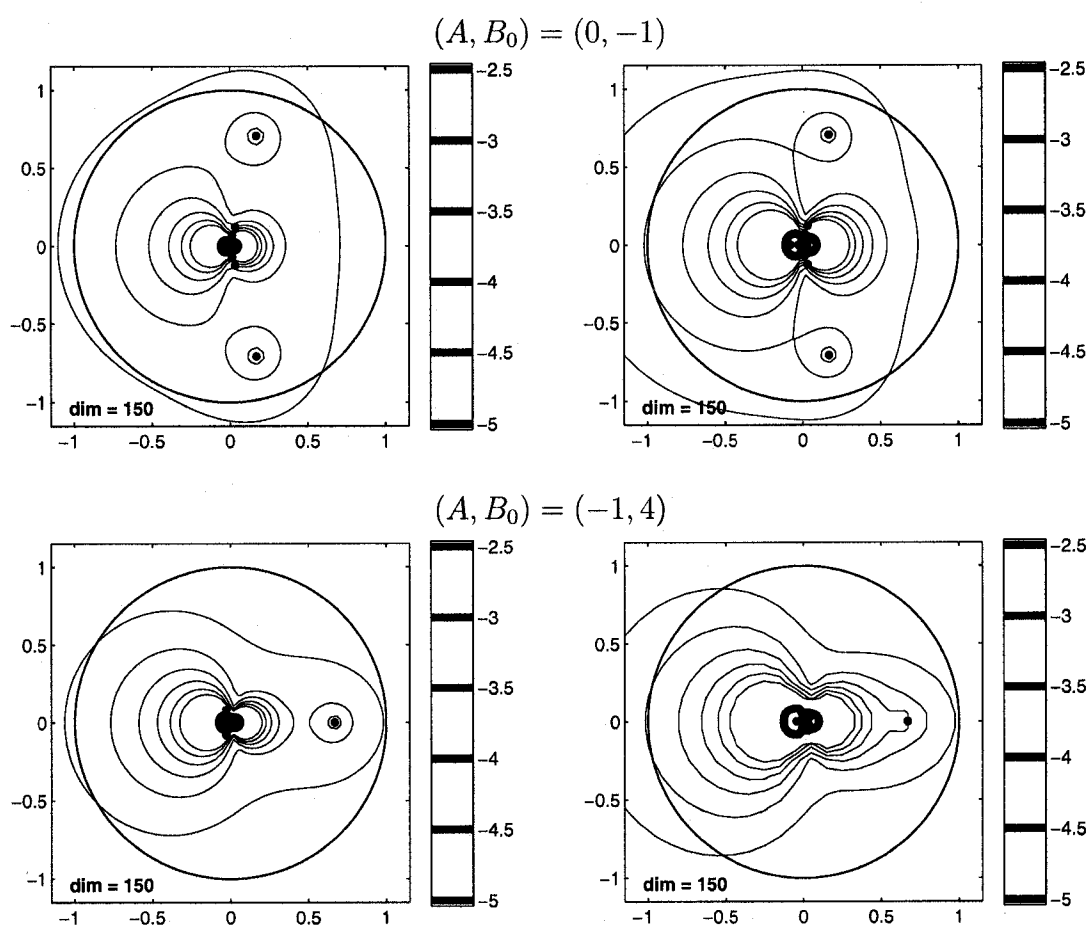which differs from p_1 by the amplitudes of its humps.

Figure 4.10 Pseudospectra for Wave Packet Perturbations for other Base
Pairs 1. This figure shows pseudospectral plots as described previously, with
base pair given above the plot. The plots on the left have delay coefficients
perturbed by $p_1(t)$ of equation (4.10) while those on the right have $p_2(t)$ as
given in equation (4.11). All show evidence of non-normality.

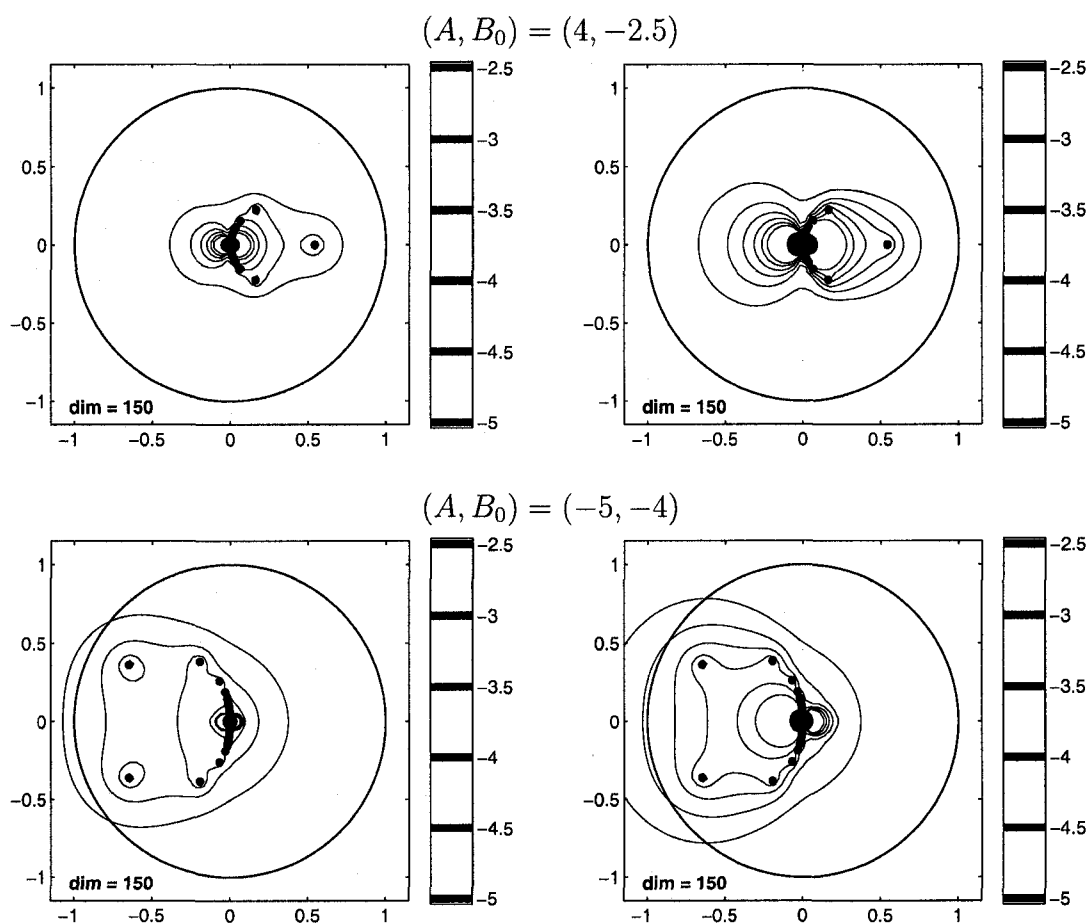$(A, B_0) = (4, -2.5)$

$(A, B_0) = (-5, -4)$

Figure 4.11 Pseudospectra for Wave Packet Perturbations for other Base Pairs 2. This figure shows pseudospectral plots as described previously. Again, there is clear evidence of non-normality for the monodromy operator approximations for DDE (4.6) with perturbed delay coefficients.

Trigonometric Perturbations

The perturbations discussed above are all localized functions in that the support is contained within a certain interval. Trigonometric functions are more global in nature, and are still of zero-mean provided, for example, that there is integer number of full waves on $[0, \tau]$. Simple functions have the form $g(t) = C_1 \sin(2\pi C_3/\tau)$ or $g(t) = C_1 \cos(2\pi C_3/\tau)$. Perturbing the delay coefficient of the DDE $\dot{y}(t) = -3.5y(t) + (-3 + g(t))y(t - 1)$ where $C_1 = 7$ and $C_3 = 5$ for these choices of $g(t)$ yields rank 150 monodromy operator approximations which exhibit non-normality. Pseudospectral plots for monodromy matrices corresponding to these perturbations is given in Figure 4.12.
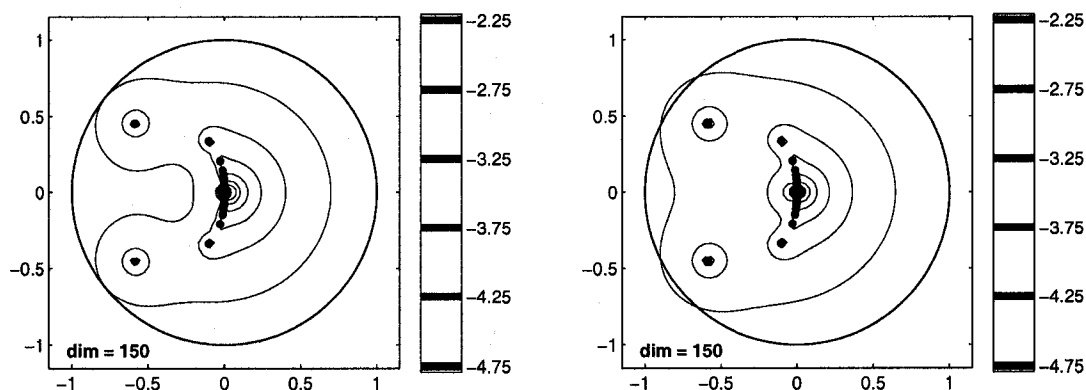

Figure 4.12 Monodromy Pseudospectra for Trigonometric Perturbation. Shown above are pseudospectral portraits for U which correspond the DDE with delay coefficient perturbed by a trigonometric functions. The left plot shows this for $g(t) = 7\sin(10\pi t)$ and the right for $g(t) = 7\cos(10\pi t)$.

The effect of trigonometric perturbations of the delay coefficient for other choices of base pairs is shown in Figures 4.13 and 4.14 shown on the following page. The figures in the left column correspond to using $g_1(t) = 10\sin(10\pi t)$ while those in the right column correspond to using $g_2(t) = 10\cos(10\pi t)$.

All pseudospectral portraits shown exhibit evidence of non-normality of the monodromy matrix U used to generated them. The level curves of the

$$(A, B_0) = (0, -1)$$

$$(A, B_0) = (-1, .4)$$

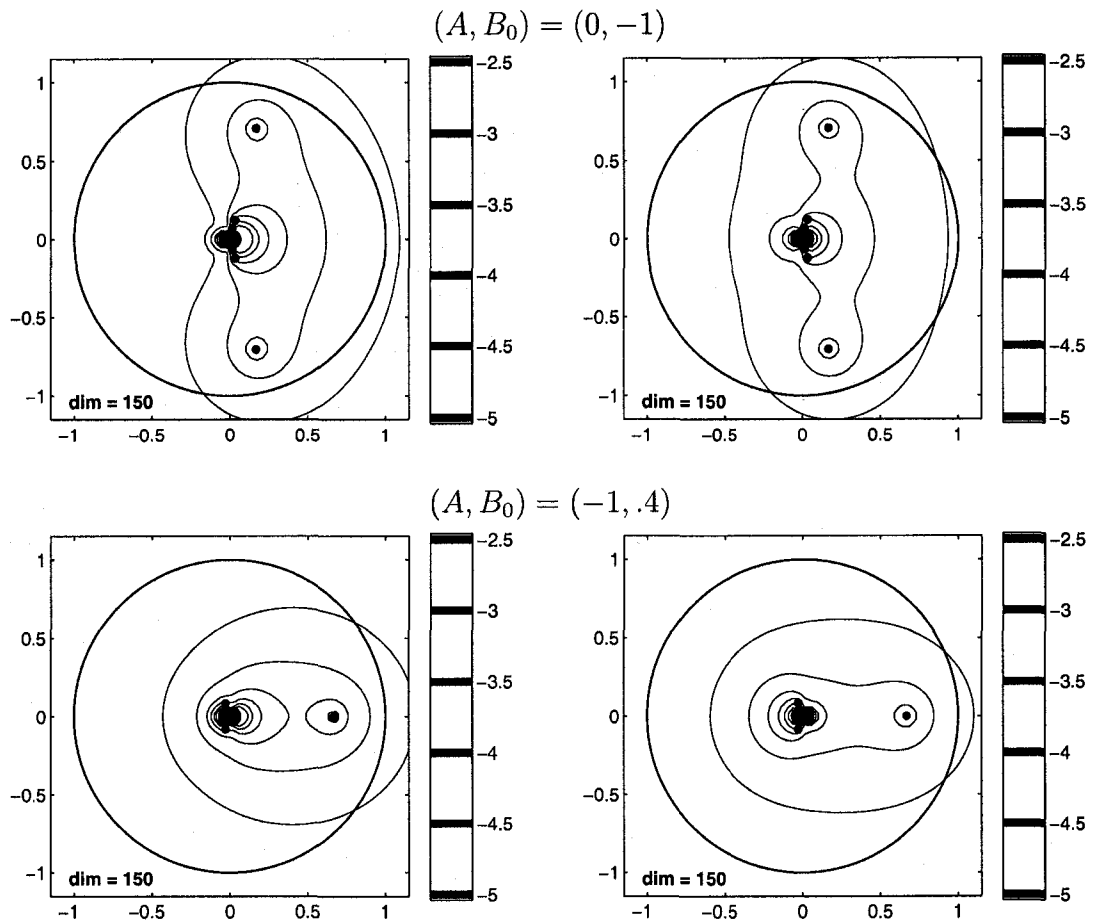

Figure 4.13 Pseudospectra for Trigonometric Perturbations of other Base Pairs 1. The figures in the left column correspond to $g_1(t) = 10\sin(10\pi t)$, and those on the right to $g_2(t) = 10\cos(10\pi t)$. The choice of base coefficients is shown centered above each pair. The unit circle is also shown.

resolvent norm in each plot differ considerably from concentric rings about the eigenvalues. In many cases, the curves leave the unit disc even though the eigenvalues may be well within the interior of it. Not addressed here are perturbations of the coefficient A, which did not induce such significant changes in the monodromy matrix as those shown above.

$$(A, B_0) = (4, -2.5)$$
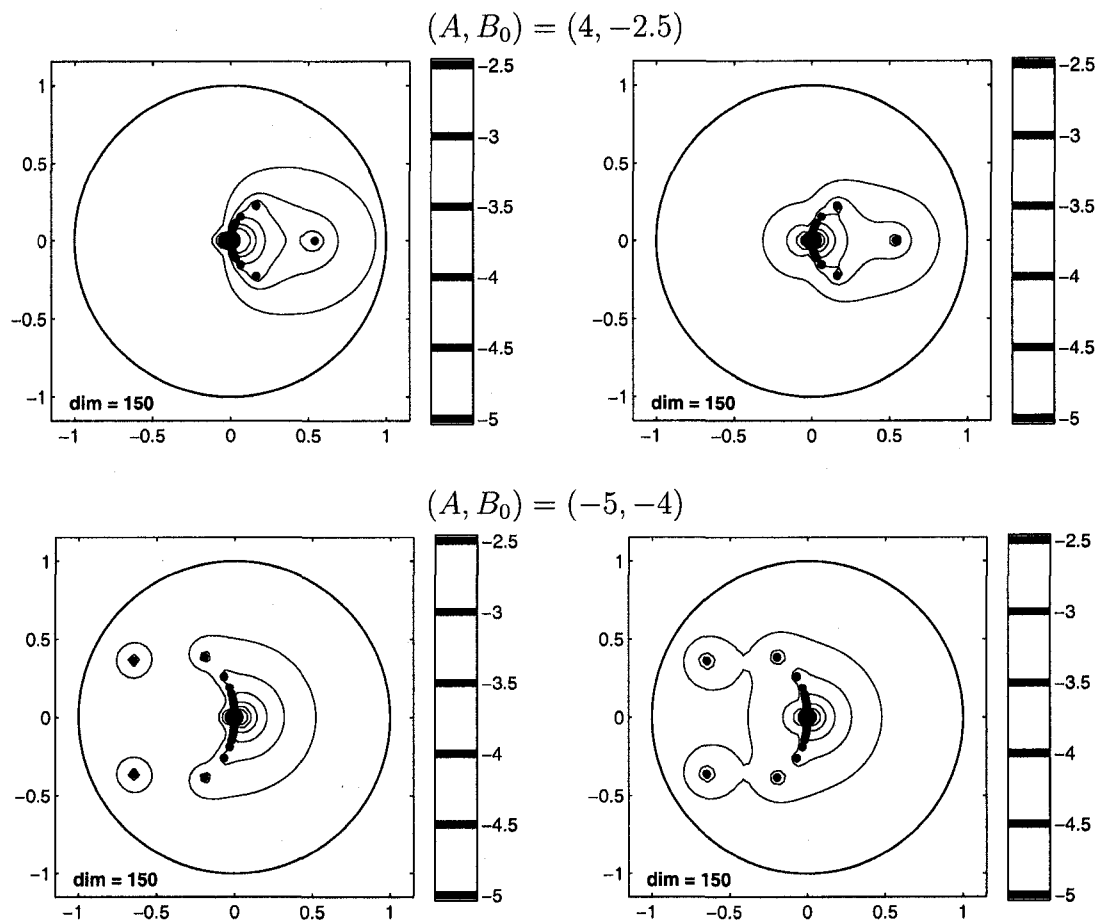

$$(A, B_0) = (-5, -4)$$

Figure 4.14 Pseudospectra for Trigonometric Perturbations of other Base Pairs 2. This figure shows pseudospectral plots as described previously. The monodromy matrices appear to be non-normal, though not to the same degree as those in the previous figure.

5 Discussion

5.1 Weight Induced Non-Normality

The monodromy operator has been defined to act on a weighted inner product space $\mathcal{H} = \mathbb{C} \oplus L^2_w[0, \tau]$, a Hilbert space in which the concept of normality is well defined. The elements of $L^2_w[0, \tau]$ are functions, normalized appropriately to account for the element $\omega \in \mathbb{C}^d$. By adjusting the size of ω in the inner product on $\mathcal{H}$, it may be possible to make the monodromy matrix U as non-normal as desired in finite dimensions.

Recall that $\omega \in \mathbb{C}^d$ represents the weight of the point-wise evaluation of the operator $\mathcal{U}$. When ω is small, the function values at $t = 0$ carry little extra significance, and an orthonormal basis for $L^2_w[0, \tau]$ is nearly an ONB for $\mathcal{H}$. However, when ω is large, the effect of the added dimension is magnified, as the function values at $t = 0$ then carry a more significant weight. An ONB for the function space $L^2_w[0, \tau]$ will also be far from normalized in that space after it is normalized in $\mathcal{H}$.

For example, consider $\{e_j\}$ to be an ONB for $L^2_w[0, \tau]$ and let e be an arbitrary representative. Denote $e_\alpha = (\alpha, e) \in \mathcal{H}$. To normalize e_α in this space, the function e_α is divided by its norm. Here,

$$\|e_\alpha\|^2_{\mathcal{H}} = \omega \alpha^2 + \|e\|_w = \omega \alpha^2 + 1 \tag{5.1}$$

so that $\widehat{e_\alpha} = \frac{e_\alpha}{\sqrt{\omega \alpha^2 + 1}}$. For large choices of ω, this renormalization has the effect of drastically resizing the basis elements $\{e_j\}$ of $L^2_w[0, \tau]$ so that they are of significantly less than unit magnitude in that space.

5.2 Growth

Recall the DDE $y(t) = -1y(t-1)$ was shown to be stable analytically. The characteristic exponents are solutions to the equation $ze^z = -1$, all of which are in the left half plane. Consequently, the Floquet multipliers are within the unit circle and the DDE is stable by either criterion. In fact, the DDE $\dot{y}(t) = \alpha y(t-1)$ is stable for any negative real choice of α. This only means that asymptotically, all solutions decay to zero. In a naive setting, one could test some choices of normalized functions ϕ by applying the monodromy operator to them a few times, and verifying that the solution begins to tend to zero.

Consider the base pair $(A, B_0) = (0, -1)$ subject to the perturbation $p(t) = 10\cos(10\pi t)$. The pseudospectra of the rank 150 monodromy matrix are shown in the upper right plot of Figure 4.14. For $\varepsilon = 10^{-2.75}$, the contour of $\Lambda_\varepsilon(U)$ extends beyond the unit circle, shown in Figure 5.1. This means that for each point z in between $\partial\mathbb{D}$ and $\Lambda_\varepsilon(U)$, there is an 'eigenvector' ψ for which z acts like an eigenvalue associated to ψ, at least for a short time. Take $z_0 = .26688 + .97512i$, which is marked in the following figure, and is clearly in the desired region. It is associated with $\varepsilon = 1.77 \cdot 10^{-3} \approx 10^{-2.7502}$.
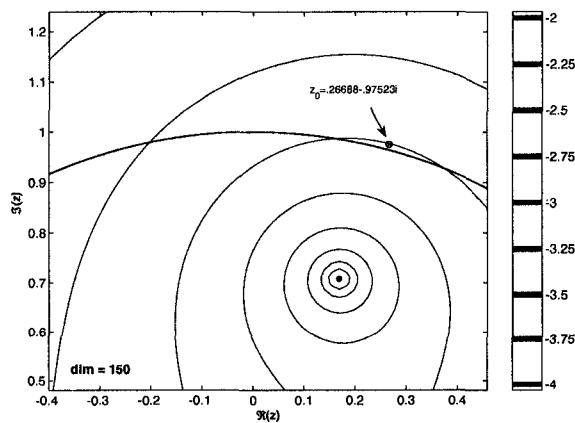

Figure 5.1 Location of Pseudoeigenvalue 1. The point $z_0 = .26688 + .97512i$ as a pseudoeigenvalue for $\varepsilon = 1.77 \cdot 10^{-3} \approx 10^{-2.7502}$.

Finding input vectors

The SVD provides a way to find an input vector associated with an element $\lambda \in \Lambda_\varepsilon(U)$ for a particular choice of ε. A note of warning: in the literature, it is customary to represent the unitary matrices of a singular value decomposition as U and V. However, U is already being used to represent approximations to the monodromy operator. Instead, Q_o and Q_i replace U and V, respectively, as the orthonormal bases for the image and preimage spaces, respectively.

Proposition 5.1 *Let $A \in \mathbb{C}^{n \times n}$ be a matrix with left singular vectors $\{q_i^j\}$ and right singular vectors $\{q_o^j\}$ where $j = 1, 2, \ldots, n$ ordered appropriately according to their corresponding singular values. Then $\|A\| = \|Aq_i^1\| = \sigma_1$.*

Proof. Take $A = Q_o \Sigma Q_i^*$ via the SVD. Since Q_i is unitary, its rows are orthonormal and its columns are the right singular vectors. In particular, the $(Q_i^* q_i^1)_j = q_i^{j*} q_i^1 = \delta_{j1}$, which means that $Q_i^* q_i^1$ is the first element of the standard basis, $I_{(:,1)}$. Applying the diagonal matrix Σ is equivalent to multiplying by σ_1, the largest singular value of A. Finally, applying Q_o to $\sigma_1 I_{:,1}$ outputs $\sigma_1 q_o^1$. This is maximal since any normalized function, v, can be written as a linear combination of $\{q_i\}$ which spans the preimage space and can be represented by a list of coefficients $\{c_j\}_1^n$ with $\sum |c_j|^2 = 1$. Note that $Q_i^* v = c$ simply vectorizes these coefficients as it writes v in the basis of its columns. Then Σc is diagonal with entries $(\Sigma c)_{jj} = \sigma_j c_j$. Finally, Q_o is unitary and preserves norm and $\|A\| = \sigma_1$, so $\sigma_1 = (\sum |\sigma_j c_j|^2)^{1/2}$ is satisfied when $c_j = 1$ and $v = q_i^1$.

∎

Corollary 5.2 *For $A \in \mathbb{C}^{n \times n}$ with the SVD given above,*

$$\inf_{x \in \mathbb{C}^n} \frac{\|Ax\|}{\|x\|} = \|Aq_i^n\| = \sigma_n \text{ and } \|A^{-1}\| = \|A^{-1} q_o^n\| = \frac{1}{\sigma_n}.$$

The goal is to find the pseudoeigenvector of $U \in \mathbb{C}^{n \times n}$ associated with the pseudoeigenvalue z_0. What is known is the point $z_0 \in \Lambda_{\varepsilon_0}(U)$ where $\varepsilon_0 > 0$ for which $\|(U - z_0 I)^{-1}\| = \varepsilon_0^{-1}$. The solution appeals to the previous corollary and the definition of the ε-pseudospectra. Recall that $\Lambda_\varepsilon(U)$ for a particular ε is the set of $z \in \mathbb{C}$ such that level curve of the resolvent norm, $\|\mathcal{R}(z, A)\|$ takes value no less than ε^{-1}. Since z_0 is chosen outside the spectrum of U and $z_0 \in \partial \Lambda_{\varepsilon_0}(U)$, this gives the inequality

$$\varepsilon^{-1} \leq \left\| (U - z_0 I)^{-1} \right\| = \varepsilon_0^{-1} < \infty \qquad (\varepsilon \geq \varepsilon_0)$$

which implies there is unit vector v giving $\|\mathcal{R}(z_0, U)v\| = \varepsilon_0$. Equivalently, there is a normalized vector $v \in \mathbb{C}^n$ such that $\|(U - z_0 I)v\| = \varepsilon_0$ and no other element of unit magnitude gives a smaller norm. By Corollary 5.2, v is the right singular value associated with the smallest singular value of the matrix $U - z_0 I$.

A Naive Algorithm

A scheme for obtaining a pseudoeigenpair (z_0, v) proceeds as follows:

1. Compute the monodromy matrix $U_0 \in \mathbb{C}^{n \times n}$ for a given set of coefficients.

2. Apply the weight matrix: $U = W U_0 W^{-1}$ to represent U_0 in a 2-norm basis.

3. Select a value $z_0 \in \Lambda_\varepsilon(U)$ for which an ε-pseudoeigenvector is desired.

4. Compute the SVD of $U - z_0 I = Q_o \Sigma Q_i^*$.

5. Take v as the last column of Q_i.

For the example point $z_0 = .26688 + .97512i$ indicated in the previous plot, the pseudoeigenvector v associated with z_0 is complex. Recall that this is a
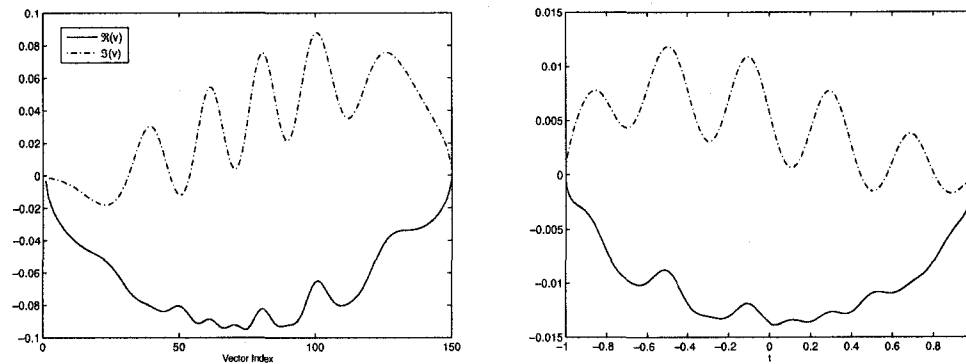
Figure 5.2 Plot of Pseudoeigenvector Associated with Pseudoeigenvalue 1.
Real and imaginary parts of the pseudoeigenvector associated with z_0 are
shown. On the left is the numerical vector associated with z_0 obtained from
the algorithm described above. On the right is the approximated history
function corresponding to this vector. This is found by aligning indices with
their appropriate Chebyshev points on the interval $[0,1]$.

normalized eigenvector, as it is the column of the unitary matrix Q_i obtained
from a SVD. The pseudoeigenvalue it is associated with has modulus only
slightly larger than 1 with $|z_0| = 1.011$, so the norm of the solution grows
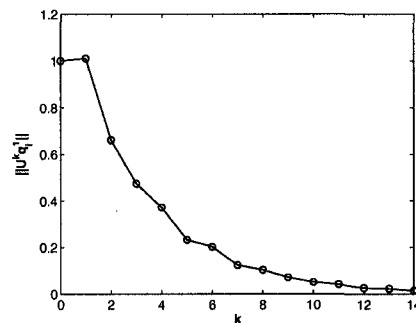slightly, shown in Figure 5.3.

Figure 5.3 Norm Powers of DDE Solution for Pseudoeigenvector 1.
Illustrated above is small transient norm growth for powers of U for the
selected input. There is no growth of the solution using only the real or
imaginary part of v, since both $\Re(z_0)$ and $\Im(z_0)$ are subunimodular.

The time evolution resulting from the real part of this pseudoeigenvector is shown in Figure 5.4. The solution to the DDE on the interval $[0, 1]$ has a different shape than the history functions supplied. This may be the result of using only the real part of the pseudoeigenvector associated with a complex pseudoeigenvalue. Note, however, that the solution on $[0, 2]$ behaves like an eigenvector associated with a negative eigenvalue on intervals of two periods.
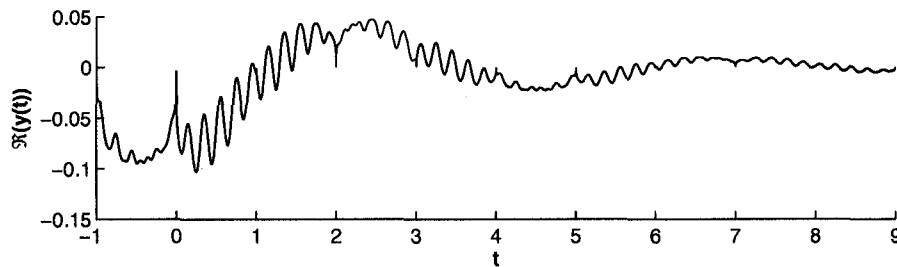

Figure 5.4 Solution to DDE for Pseudoeigenvector 1. Real part of the solution to $\ddot{y}(t) = (-1 + 10\cos(10\pi t))y(t - 1)$ with the history function depicted in the right plot of Figure 5.2, shown on $t \in [-1, 0)$.

The weakness of the previous example was that the eigenvalue nearest the point z_0 is almost purely imaginary, and so the eigenvector associated with it had a large imaginary component, which influenced much of the growth by changing signs under successive powers.

Consider a second DDE $\ddot{y}(t) = -5y(t) + [-4 + p_1(t)]y(t - 1)$ where $p_1(t)$ of the form of superimposed wave packets given in Equation (4.10). A portion of the bottom left plot of Figure 4.10 is reproduced in Figure 5.5 showing the location of an ε-pseudoeigenvalue for $\varepsilon \approx 10^{-2.5}$.

Since $z_1 = -1.1$ is a purely real pseudoeigenvalue, and U is a real matrix, it is expected that its pseudoeigenvector is also real. Growth is again expected as $|z_1| > 1$.

The solution to the DDE, shown in the bottom plot of Figure 5.6 with this vector as the history vector demonstrates the DDE behaves as though it is
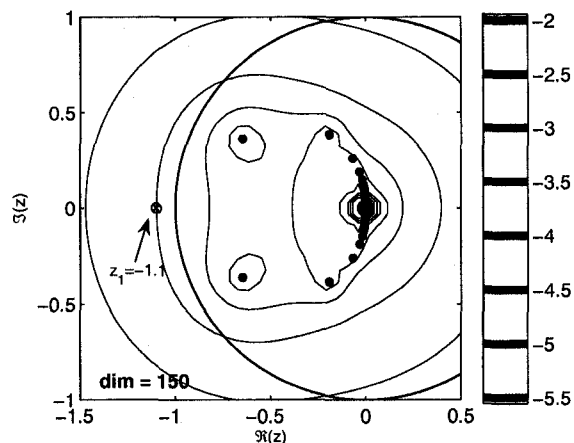
Figure 5.5 Location of Pseudoeigenvalue 2. The point $z_1 = -1.1$ is chosen as a pseudoeigenvalue of U where the delay coefficient is perturbed by (4.10). The ε associated with z_1 is approximately $10^{-2.5}$.

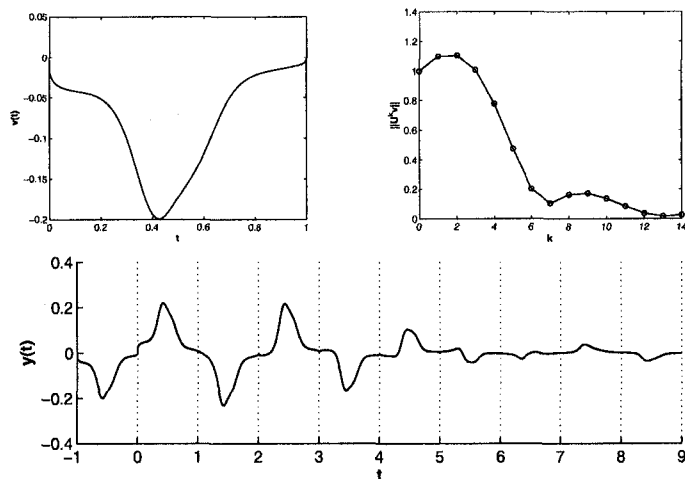nearly in an eigenstate. It also shows amplification before beginning to decay.

Figure 5.6 Plot and Norm Powers under U for Pseudoeigenvector 2. The pseudoeigenvector v associated to $z_1 = -1.1$ is shown in the top left plot, and norm powers $\left\| U^k v \right\|_2$ in the top right plot. The corresponding computed solution to $\ddot{y}(t) = -5y(t) - (4 + p_1(t))y(t - 1)$ is shown in the lower plot.

An issue which will now be addressed is the extent to which the rank of the approximation to $\mathcal{U}$ affects the pseudoeigenvector and solution found

above. Numerical evidence suggests that the size of the monodromy matrix does not affect the numerical solution, up to a constant dependent on the size of U. Shown below in Figure 5.7 is the solution shown in the lower plot of Figure 5.6 for monodromy matrices of rank $n = 30, 50, 100$, and 200. The shape of the solution does not change. The input vector is taken as the smallest singular vector of $WUW^{-1} + 1.1I$ where U, I, and W all depend on n. They are nearly identical, up to scaling. Normalizing each history vector equally would account for this scale factor. This demonstrates that the results of examples conducted with $n = 150$ should remain the same for other choices of n.

A final example shows the behavior of a DDE to a history function taken to be a pseudoeigenvector associated with a positive real pseudoeigenvalue
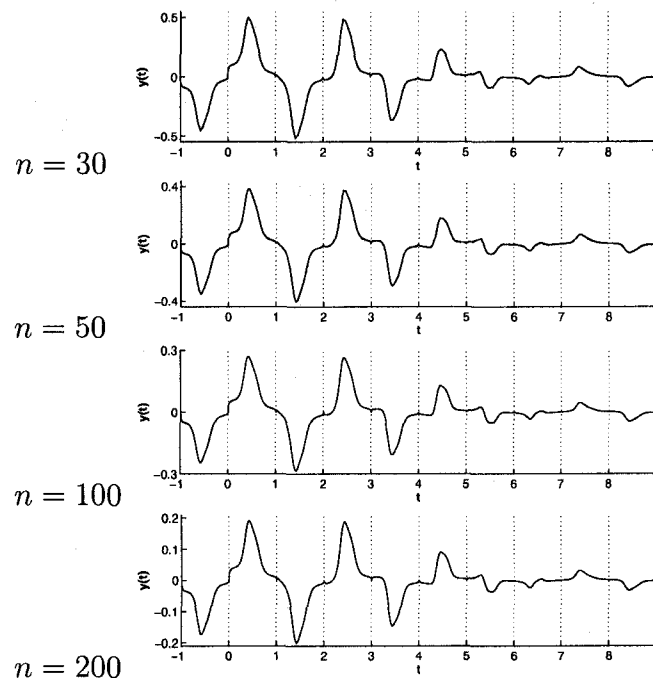

Figure 5.7 Solution to a DDE, Computed by Matrices of Different Rank. Displayed here are solutions to $\ddot{y}(t) = -5y(t) + [-4 + p(t)]y(t-1)$ with $p(t)$ given in (4.10) using monodromy matrices of various ranks, given on the left. The history function used is the pseudoeigenvector associated to $z = -1.1$, obtained using U. The solutions appear identical up to scaling.

outside the unit circle. The DDE

$$\dot{y}(t) = -y(t) + \left(\frac{1}{2} + 10\sin(10\pi t)\right)y(t-1) \qquad (5.2)$$

has a pseudoeigenvalue at $z_2 = 1.24$ for $\varepsilon \approx 10^{-2.5}$. Shown below are the pseudoeigenvector, v, the norms of powers of the weighted matrix for this input, and a plot of the solution the DDE with v as an initial condition. Again, as in all instances discussed in this section so far, $\mathcal{U}$ is approximated by a rank 150 matrix.
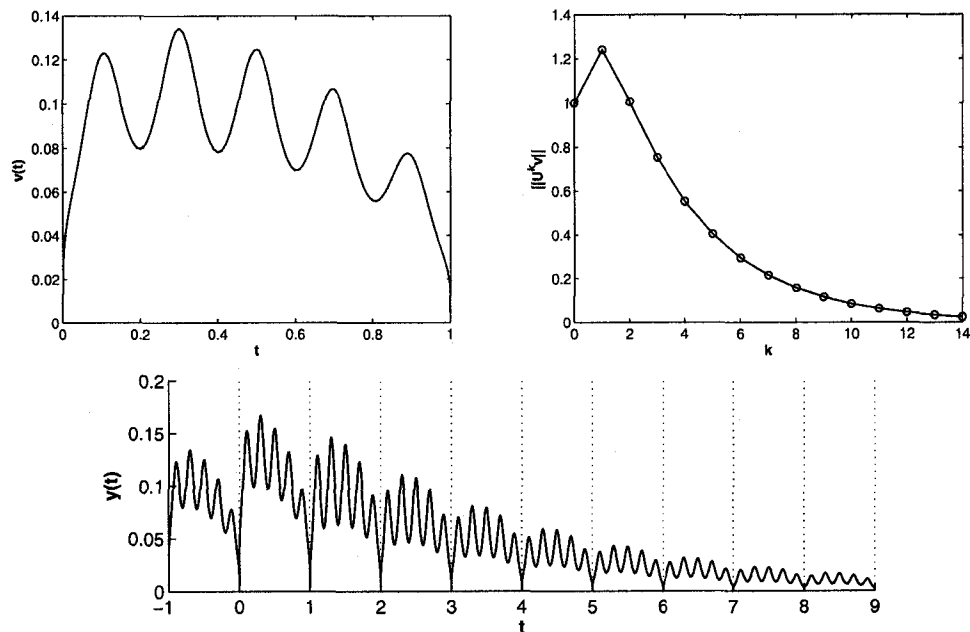

Figure 5.8 Pseudoeigenvector, Transient Growth, and Solution for DDE (5.2). Pseudoeigenvector (top left), norms of powers (top right), and solution (bottom) for the DDE of Equation (5.2) for pseudoeigenvalue $z_2 = 1.24$.

The initial transient growth in these simple examples is quickly damped out over a few iterations. However, it is possible for growth to continue for an extended period of time. This is demonstrated in cases when there is a numerous collection of large eigenvalues even though all are within the unit circle.

However, to find examples in which there are many large eigenvalues, it is necessary to select base pairs (A, B_0) which are far from the origin. For base pairs inside the stability region for scalar DDEs, this amounts to taking A to be a large negative number such as $A = -200$. The numerical scheme then uses the fundamental matrix solution to the very stiff ODE $\dot{y}(t) = -200y(t)$ to approximate $\mathcal{U}$. It may be difficult to assess the accuracy of U in this case, so an example of this type is not explored.

5.3 Final Remarks

This thesis has demonstrated that non-normality can appear in monodromy operators associated with scalar linear periodic-coefficient delay differential equations in one dimension. The concept of normality applies in a strict sense to objects acting on inner-product spaces. By choosing an inner product on functions of t, non-normality of the monodromy operator $\mathcal{U}$ for a DDE, and of its matrix approximation, may be investigated. It was demonstrated that for certain DDEs, choices of time-dependent coefficients affect the normality of finite rank approximations to the monodromy operator $\mathcal{U}$. As these matrices are spectral approximations of a Hilbert space operator which is compact, the accuracy of the finite rank matrices with regard to eigenvalues and eigenvectors implies the normality of matrix approximations well represent the normality of the operator.

Some shortcomings of this approach are the lack of usefulness of the eigenvector matrix condition number as an accurate measure of non-normality. Due to compact operators' spectral structure and the numerical methods used, high rank approximations of the monodromy operator produce a large number of inaccurate eigenvalues. Although these have little bearing on questions such as stability, each is associated with an eigenvector of questionable accuracy. This produces, it is suspected, unusually large eigenvector matrix

condition numbers for the demonstrated behavior of the monodromy matrix.

Non-normality, instead, was demonstrated by computing ε-pseudospectra, and through growth of selected inputs for stable matrices which are not accounted for by eigenvalues alone.

It remains unclear what properties of $p(t)$, applied to the delay coefficient of a constant coefficient DDE, induce non-normality. Reflection on the shape of the pseudoeigenvectors in Figures 5.2 and 5.8 suggests that a relation exists between the type of delay coefficient perturbation and this vector. Perturbations of the delay coefficient have the effect of altering the eigenvectors of U, and understanding this connection more clearly is an appropriate topic for further research.

List of References

[1] András Bátkai and Susanna Piazzera, *Semigroups for delay equations*, Research Notes in Mathematics, vol. 10, A K Peters Ltd., Wellesley, MA, 2005.

[2] Alfredo Bellen and Marino Zennaro, *Numerical methods for delay differential equations*, Numerical Mathematics and Scientific Computation, The Clarendon Press Oxford University Press, New York, 2003.

[3] Richard Bellman, *Introduction to matrix analysis*, Classics in Applied Mathematics, vol. 19, Society for Industrial and Applied Mathematics (SIAM), Philadelphia, PA, 1997.

[4] Richard Bellman and Kenneth L. Cooke, *Differential-difference equations*, Academic Press, New York, 1963.

[5] Abraham Berman, Michael Neumann, and Ronald J. Stern, *Nonnegative matrices in dynamic systems*, Pure and Applied Mathematics (New York), John Wiley & Sons Inc., New York, 1989.

[6] Jean-Paul Berrut and Lloyd N. Trefethen, *Barycentric Lagrange interpolation*, SIAM Review **46** (2004), no. 3, 501–517.

[7] Béla Bollobás, *Linear analysis: An introductory course*, Press Synidicate of the University of Cambridge, 1990.

[8] Ed Bueler, *Chebyshev collocation for linear, periodic ordinary and delay differential equations: a posteriori estimates*, (2004), http://www.citebase.org/abstract?id=oai:arXiv.org:math/0409464.

[9] _____, *Guide to ddec: stability of linear, periodic ddes using the ddec suite*, (2005), http://www.uaf.edu/ bueler/ddectutor.pdf.

[10] Ed Bueler and Eric Butcher, *Stability of periodic linear delay-differential equations and the Chebyshev approximation of fundamental solutions*, Tech. Report Technical Report 02-03, Department of Mathematical Sciences, University of Alaska Fairbanks, 2002.

[11] Eric A. Butcher, Haitao Ma, Ed Bueler, Victoria Averina, and Zsolt Szabo, *Stability of linear time-periodic delay-differential equations via Chebyshev polynomials*, Internat. J. Numer. Methods Engrg. **59** (2004), no. 7, 895–922.

[12] Ward Cheney and David Kincaid, *Numerical mathematics and computing*, Brooks/Cole Publishing Co., Monterey, Calif., 1980, Contemporary Undergraduate Mathematics Series.

[13] Carmen Chicone, *Ordinary differential equations with applications*, Texts in Applied Mathematics, vol. 34, Springer-Verlag, New York, 1999.

[14] R. M. Corless, G. H. Gonnet, D. E. G. Hare, D. J. Jeffrey, and D. E. Knuth, *On the Lambert W function*, Adv. Comput. Math. **5** (1996), no. 4, 329–359.

[15] J.K. Cullum and A.E. Ruehli, *Pseudospectra analysis, nonlinear eigenvalue problems, and studying linear systems wiht delays*, BIT **41** (2001), no. 2, 265–282.

[16] E. B. Davies, *Spectral theory and differential operators*, Cambridge Studies in Advanced Mathematics, vol. 42, Cambridge University Press, Cambridge, 1995.

[17] Wai Sun Don and David Gottlieb, *The Chebyshev-Legendre method: implementing Legendre methods on Chebyshev points*, SIAM J. Numer. Anal. **31** (1994), no. 6, 1519–1534.

[18] R. D. Driver, *Ordinary and delay differential equations*, Springer-Verlag, New York, 1977.

[19] J. Doyne Farmer, *Chaotic attractors of an infinite-dimensional dynamical system*, Phys. D **4** (1981/82), no. 3, 366–393.

[20] Călin-Ioan Gheorghiu, *On the scalar measure of non-normality of matrices—dimension vs. structure*, Gen. Math. **11** (2003), no. 1-2, 21–32.

[21] David E. Gilsinn and Florian A. Potra, *Integral operators and delay differential equations*, J. Integral Equations Appl. **18** (Fall 2006), no. 3, 297–336.

[22] Gene H. Golub and Charles F. Van Loan, *Matrix computations*, Johns Hopkins Studies in the Mathematical Sciences, Johns Hopkins University Press, Baltimore, MD, 1996.

[23] Kirk Green and Thomas Wagenknecht, *Pseudospectra and delay differential equations*, J. Comput. Appl. Math. **196** (2006), no. 2, 567–578.

[24] Karl E. Gustafson and Duggirala K. M. Rao, *Numerical range*, Universitext, Springer-Verlag, New York, 1997, The field of values of linear operators and matrices.

[25] Jack K. Hale, *Ordinary differential equations*, Robert E. Krieger Publishing Co. Inc., Huntington, N.Y., 1980.

[26] Kenneth B. Hannsgen, Terry L. Herdman, Harlan W. Stech, and Robert L. Wheeler (eds.), *Volterra and functional-differential equations*, Lecture Notes in Pure and Applied Mathematics, vol. 81, Marcel Dekker Inc., New York, 1982.

[27] Nicholas J. Higham, *The numerical stability of barycentric lagrange interpolation*, IMA Journal of Numerical Analysis **24** (2004), 547–556.

[28] D. W. Jordan and P. Smith, *Nonlinear ordinary differential equations*, Oxford Texts in Applied and Engineering Mathematics, vol. 2, Oxford University Press, Oxford, 1999.

[29] Tosio Kato, *Perturbation theory for linear operators*, Classics in Mathematics, Springer-Verlag, Berlin, 1995.

[30] Ju. S. Kolesov and D. I. Švitra, *The role of time-delay in mathematical models of ecology*, Litovsk. Mat. Sb. **19** (1979), no. 1, 115–128, 231.

[31] Bernd Krauskopf and Kirk Green, *Computing unstable manifolds of periodic orbits in delay differential equations*, J. Comput. Phys. **186** (2003), no. 1, 230–249.

[32] Yang Kuang, *Delay differential equations with applications in population dynamics*, Mathematics in Science and Engineering, vol. 191, Academic Press Inc., Boston, MA, 1993.

[33] Wilhelm Magnus, *On the exponential solution of differential equations for a linear operator*, Comm. Pure Appl. Math. **7** (1954), 649–673.

[34] Marc R. Roussel, *The use of delay differential equations in chemical kinetics*, J. Phys. Chem. **100** (1996), no. 20, 8323–8330.

[35] W. Rudin, *Real and complex analysis*, McGraw-Hill, New York, 1974.

[36] Eitan Tadmor, *The exponential accuracy of Fourier and Chebyshev differencing methods*, SIAM J. Numer. Anal. **23** (1986), no. 1, 1–10.

[37] Lloyd N. Trefethen, *Computation of pseudospectra*, Acta numerica, 1999, Acta Numer., vol. 8, Cambridge Univ. Press, Cambridge, 1999, pp. 247–295.

[38] _____, *Spectral methods in MATLAB*, Software, Environments, and Tools, Society for Industrial and Applied Mathematics (SIAM), Philadelphia, PA, 2000.

[39] Lloyd N. Trefethen and David Bau, III, *Numerical linear algebra*, Society for Industrial and Applied Mathematics (SIAM), Philadelphia, PA, 1997.

[40] Lloyd N. Trefethen and Mark Embree, *Spectra and pseudospectra*, Princeton University Press, Princeton, NJ, 2005.

[41] Thomas G. Wright, `Eigtool`, http://www.comlab.ox.ac.uk/pspectra/eigtool/ (2005).

[42] Thomas G. Wright and Lloyd N. Trefethen, *Pseudospectra of rectangular matrices*, IMA J. Numer. Anal. **22** (2002), no. 4, 501–519.